A Geometric View of Optimal Transportation and Generative Adversarial Networks (GANs)

Shing-Tung Yau[1]

[1]Center of Mathematical Sciences and Applications
Harvard University

Microsoft, Seattle

Collaborators

These projects are collaborated with David Gu and many other mathematicians, computer scientists.

Outline

1. Manifold Distribution Hypothesis
2. Manifold learning
3. Overview of Optimal transportation
4. Collaboration vs. competition between generators and discriminator
5. Regularity and mode collapse
6. Autoencoder-Optimal Transport framework

Manifold Distribution Hypothesis

Why dose DL work?

Deep learning is the mainstream technique for many machine learning tasks, including image recognition, machine translation, speech recognition, and so on. Despite its success, the theoretical understanding on how it works remains primitive.

Manifold Distribution Hypothesis

We believe the great success of deep learning can be partially explained by the well accepted manifold distribution and the clustering distribution hypothesis:

Manifold Distribution

Natural high dimensional data concentrates close to a non-linear low-dimensional manifold.

Clustering Distribution

The distances among the probability distributions of subclasses on the manifold are far enough to discriminate them.

Deep learning method can learn and represent the manifold structure, and transform the probability distributions.

MNIST tSNE Embedding

a. LeCunn's MNIST handwritten digits samples on manifold

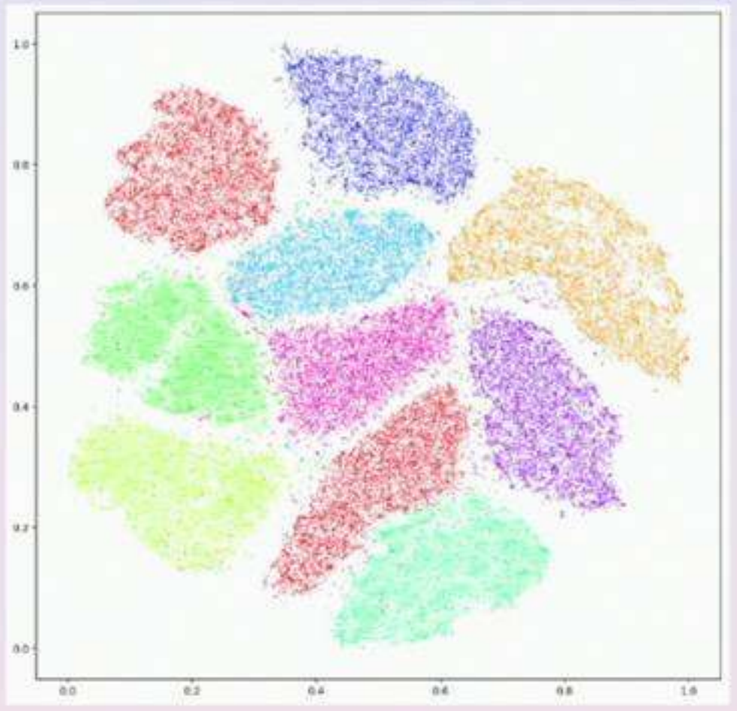

b. Hinton's t-SNE embemdding on latent space

- Each image 28×28 is treated as a point in the image space $\mathbb{R}^{28\times 28}$;
- The hand-written digits image manifold is only two dimensional;
- Each digit corresponds to a distribution on the manifold.

MNIST Siamese Embedding

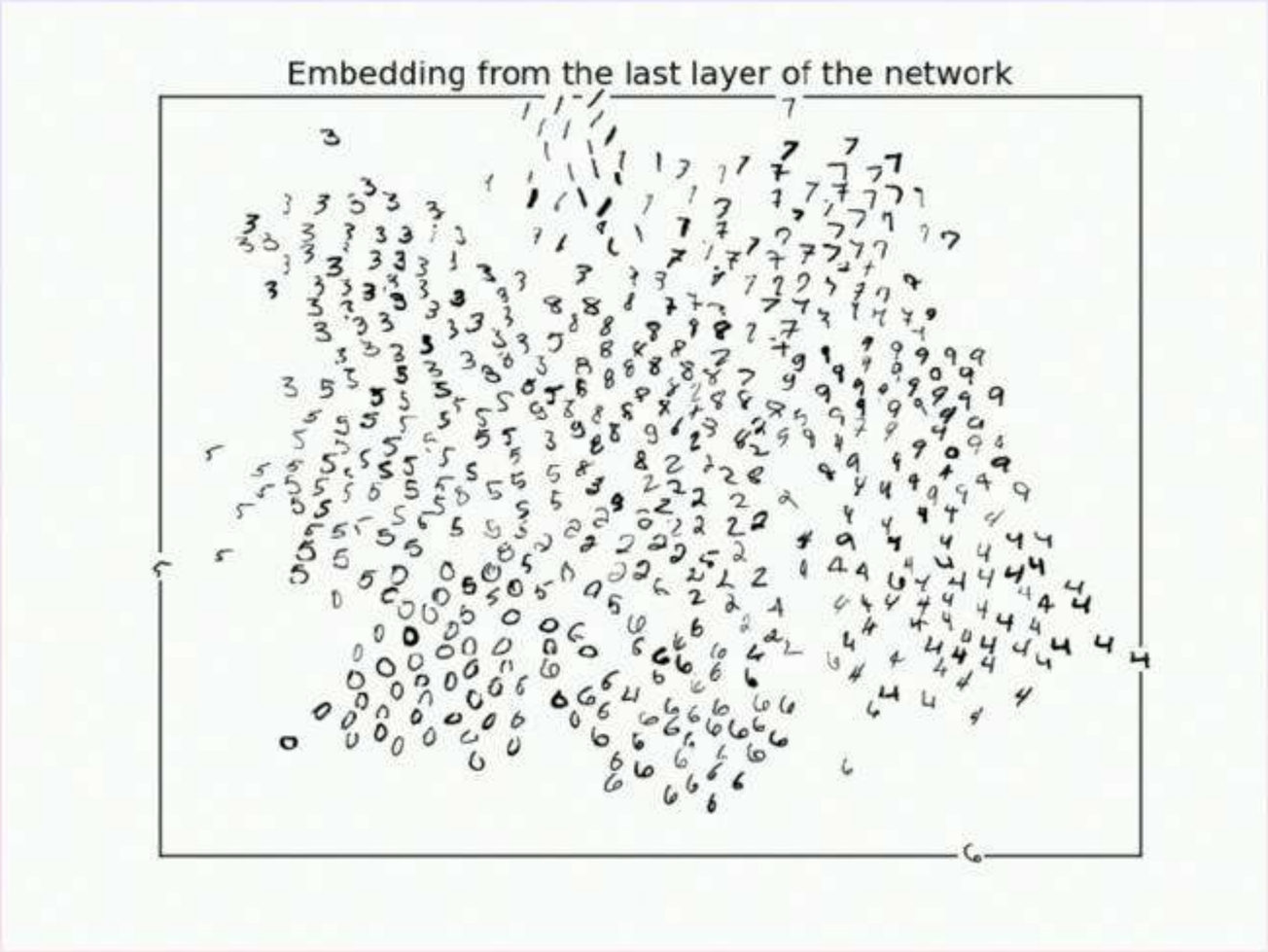

Different embedding result with inferior quality by a Siamese network.

General Model

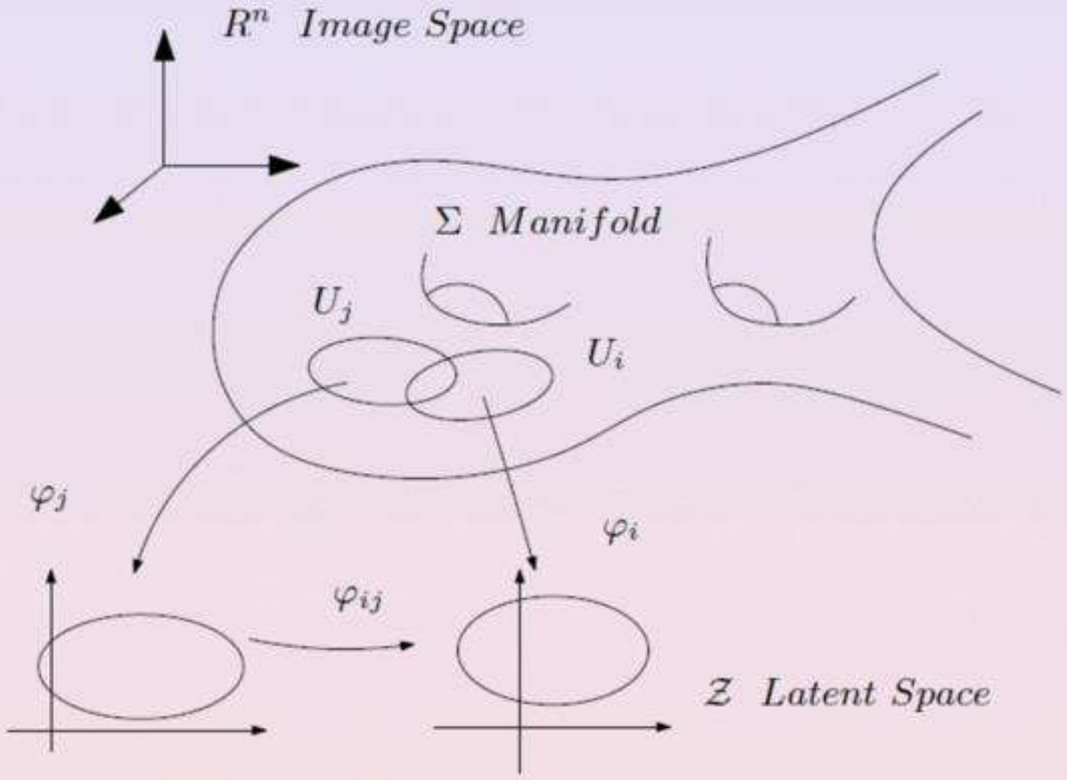

- Ambient Space- image space $\mathbb{R}^n$
- manifold - Support of a distribution μ
- parameter domain - latent space $\mathbb{R}^m$
- coordinates map φ_i- encoding/decoding maps
- φ_{ij} controls the probability measure

Manifold Structure

Definition (Manifold)

Suppose M is a topological space, covered by a set of open sets $M \subset \bigcup_\alpha U_\alpha$. For each open set U_α, there is a homeomorphism $\varphi_\alpha : U_\alpha \to \mathbb{R}^n$, the pair $(U_\alpha, \varphi_\alpha)$ form a chart. The union of charts form an atlas $\mathscr{A} = \{(U_\alpha, \varphi_\alpha)\}$. If $U_\alpha \cap U_\beta \neq \emptyset$, then the chart transition map is given by

$$\varphi_{\alpha\beta} : \varphi_\alpha(U_\alpha \cap U_\beta) \to \varphi_\beta(U_\alpha \cap U_\beta),$$

$$\varphi_{\alpha\beta} := \varphi_\beta \circ \varphi_\alpha^{-1}.$$

Example

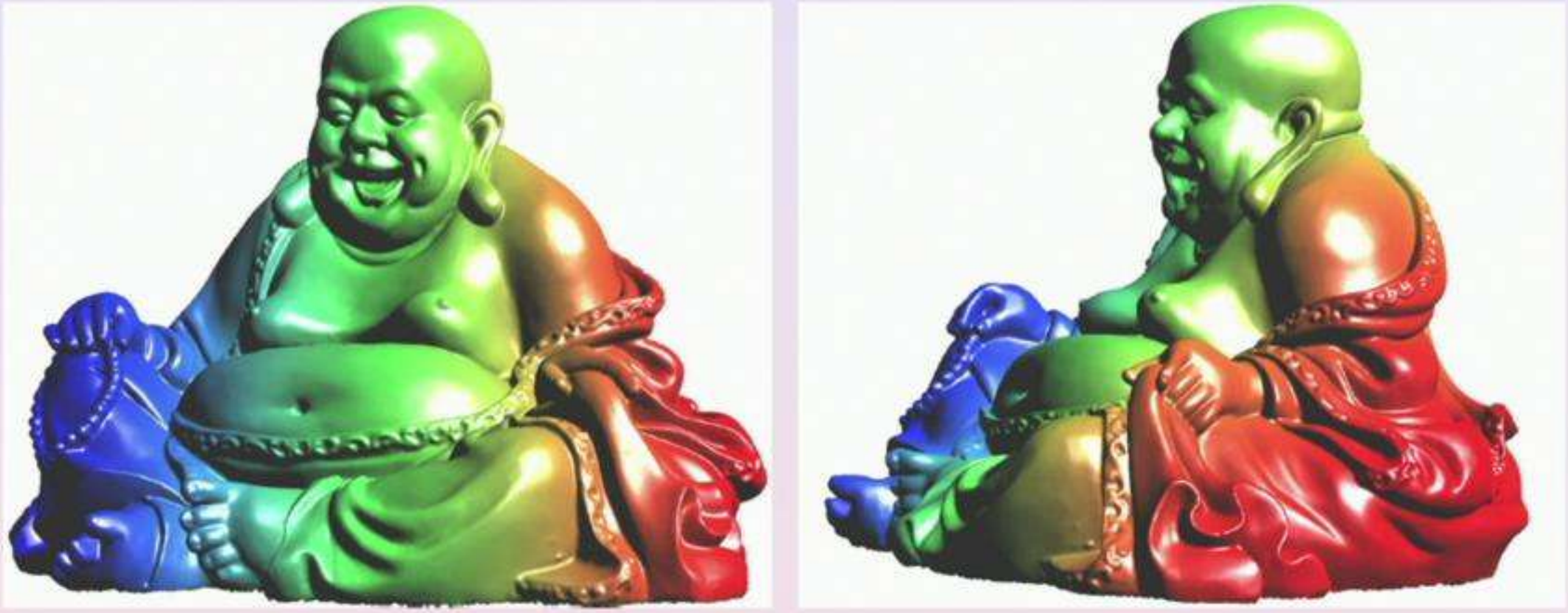

Image space $\mathscr{X}$ is $\mathbb{R}^3$; the data manifold Σ is the happy buddaha.

Example

The encoding map is $\varphi_i : \Sigma \to \mathscr{Z}$; the decoding map is $\varphi_i^{-1} : \mathscr{Z} \to \Sigma$.

Example

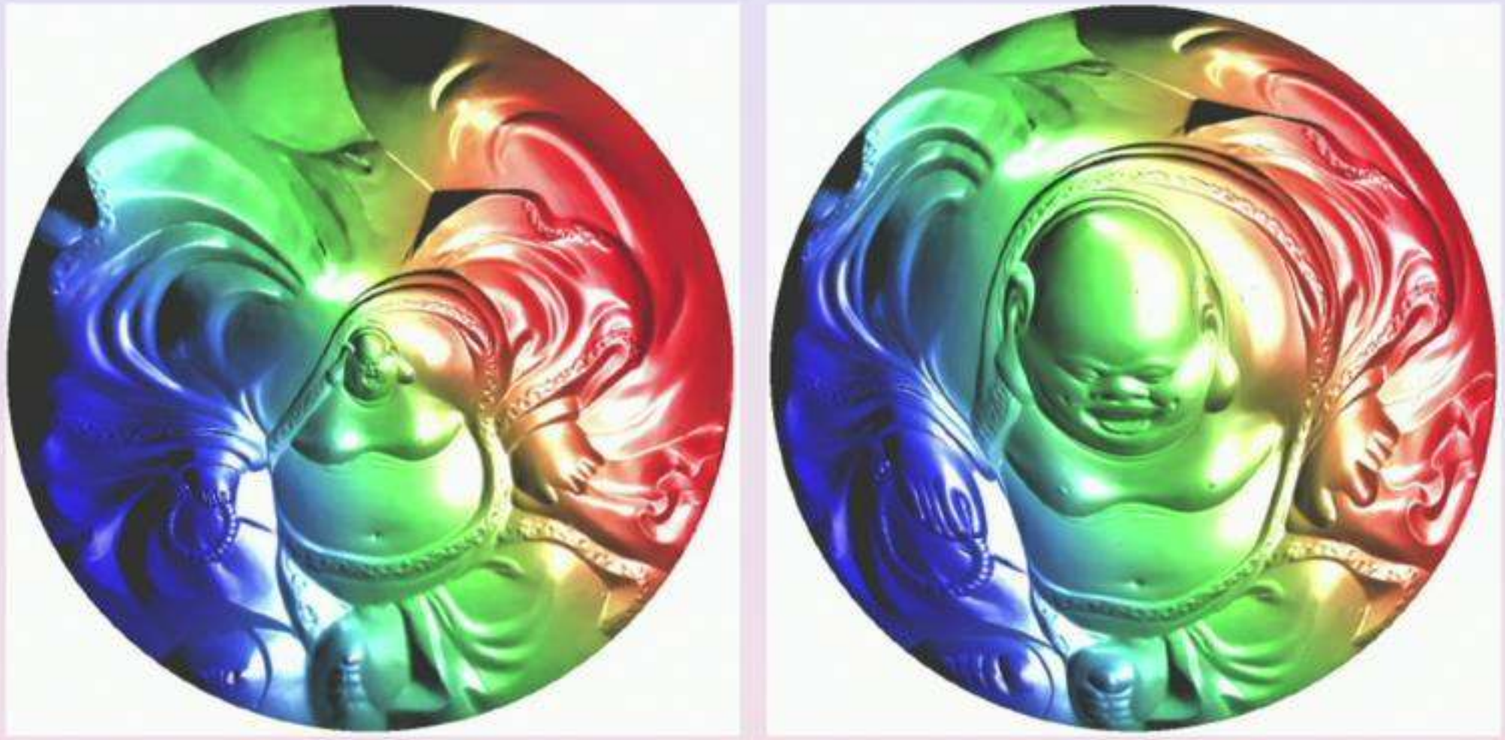

The automorphism of the latent space $\varphi_{ij} : \mathscr{Z} \to \mathscr{Z}$ is the chart transition.

Example

Uniform distribution ζ on the latent space $\mathscr{Z}$, non-uniform distribution on Σ produced by a decoding map.

Example

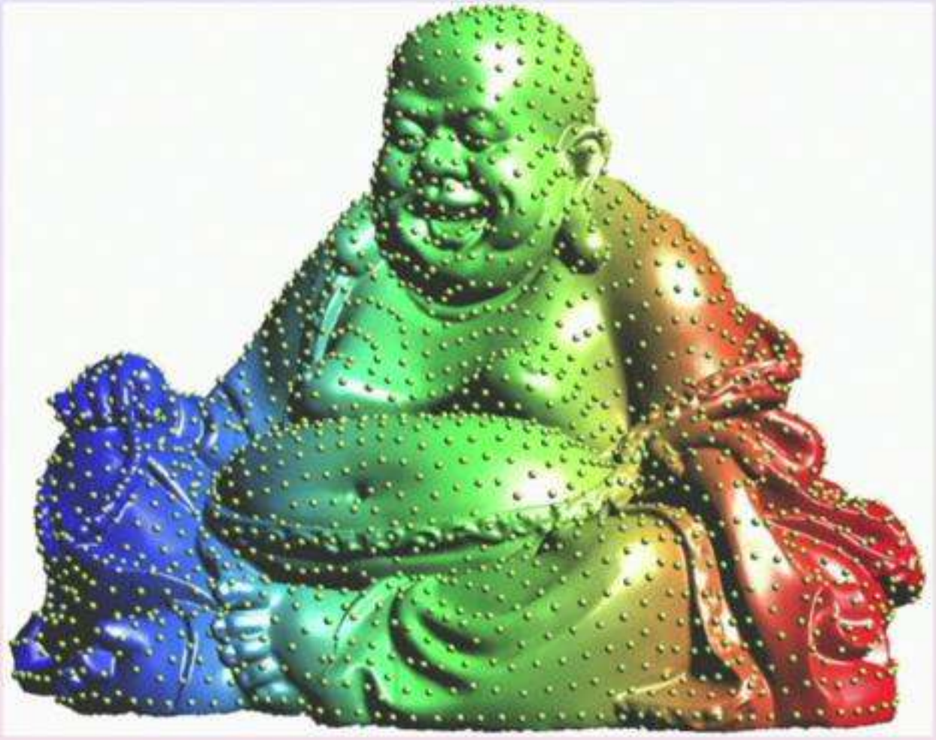

Uniform distribution ζ on the latent space $\mathscr{Z}$, uniform distribution on Σ produced by another decoding map.

Example

Uniform distribution ζ on the latent space $\mathscr{Z}$, non-uniform distribution on Σ produced by a decoding map.

Example

Uniform distribution ζ on the latent space $\mathscr{Z}$, uniform distribution on Σ produced by another decoding map.

Human Facial Image Manifold

One facial image is determined by a finite number of genes, lighting conditions, camera parameters, therefore all facial images form a manifold.

Manifold view of Generative Model

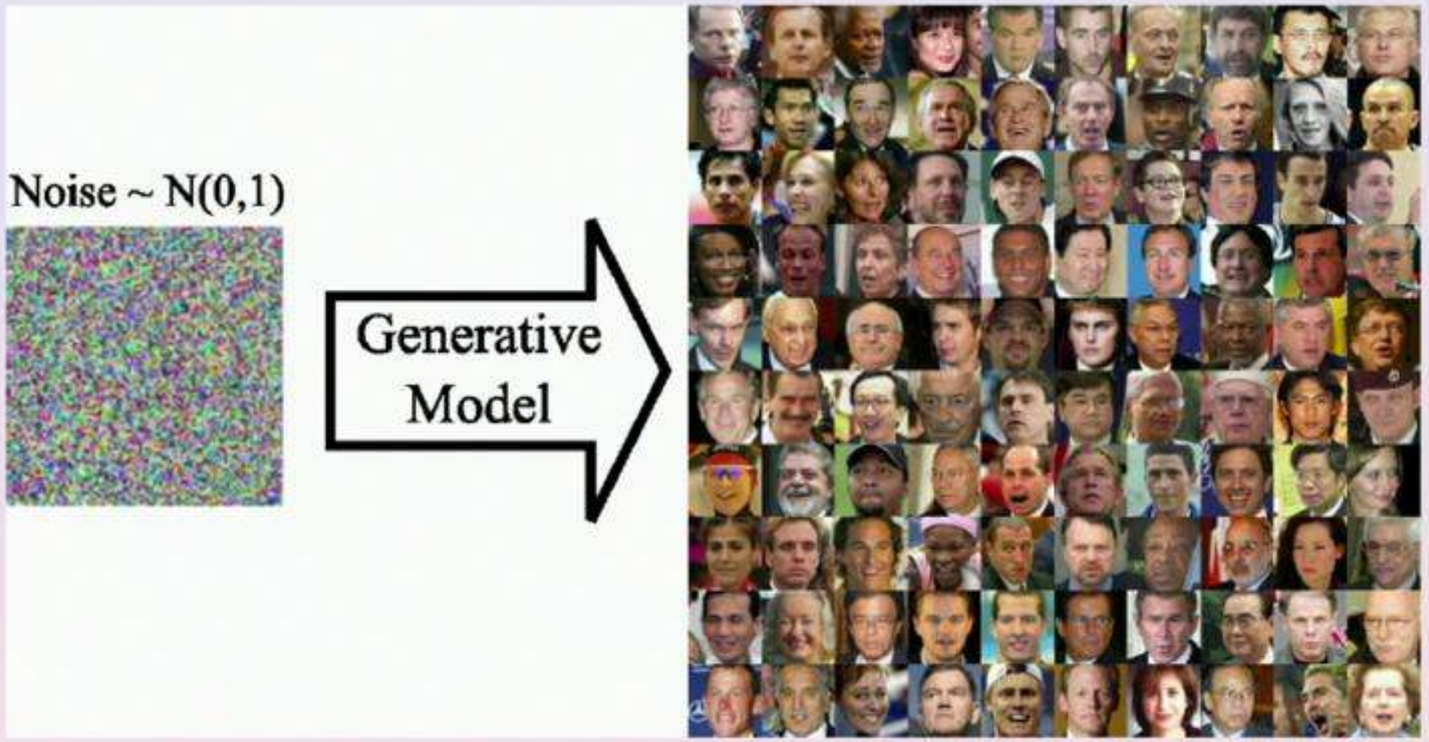

Given a parametric representation $\varphi : \mathscr{Z} \to \Sigma$, randomly generate a parameter $z \in \mathscr{Z}$ (white noise), $\varphi(z) \in \Sigma$ is a human facial image.

Manifold view of Denoising

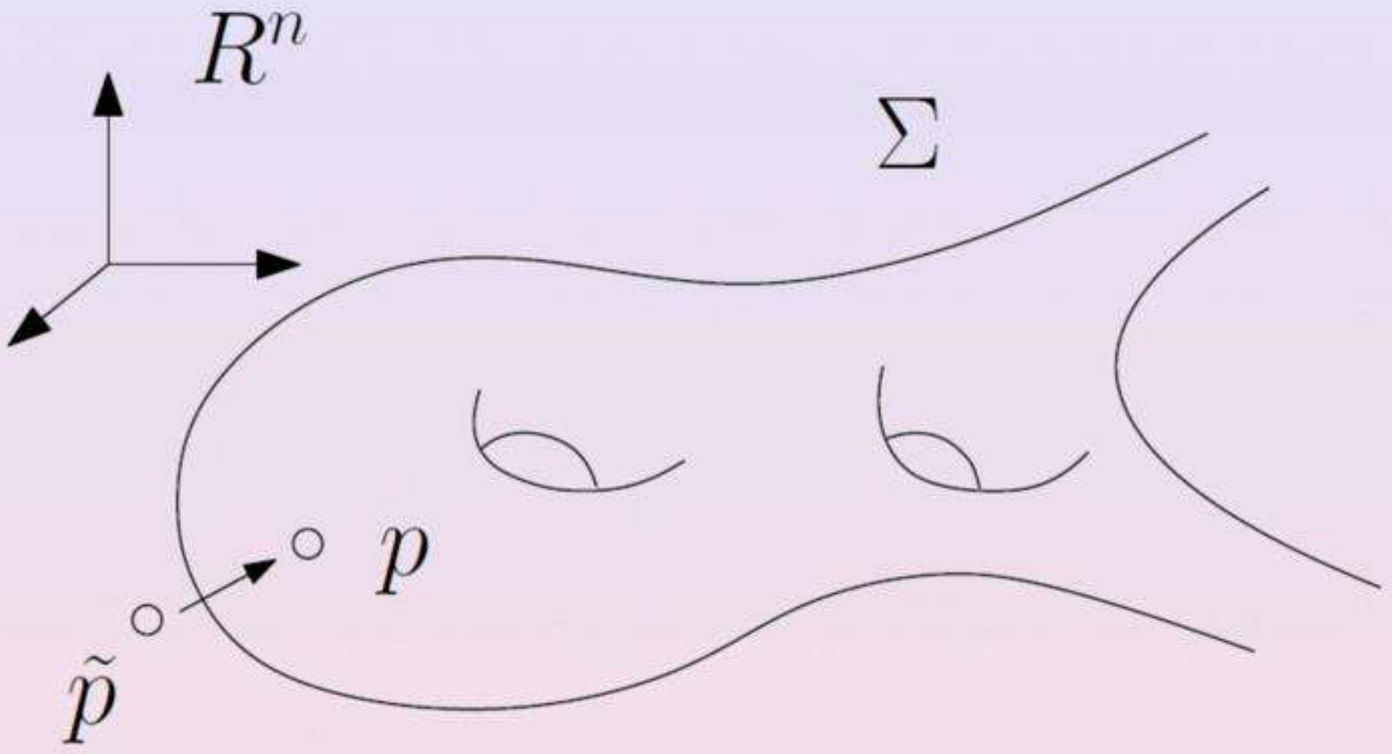

Suppose $\tilde{p}$ is a point close to the manifold, $p \in \Sigma$ is the closest point of $\tilde{p}$. The projection $\tilde{p} \to p$ can be treated as denoising.

Manifold view of Denoising

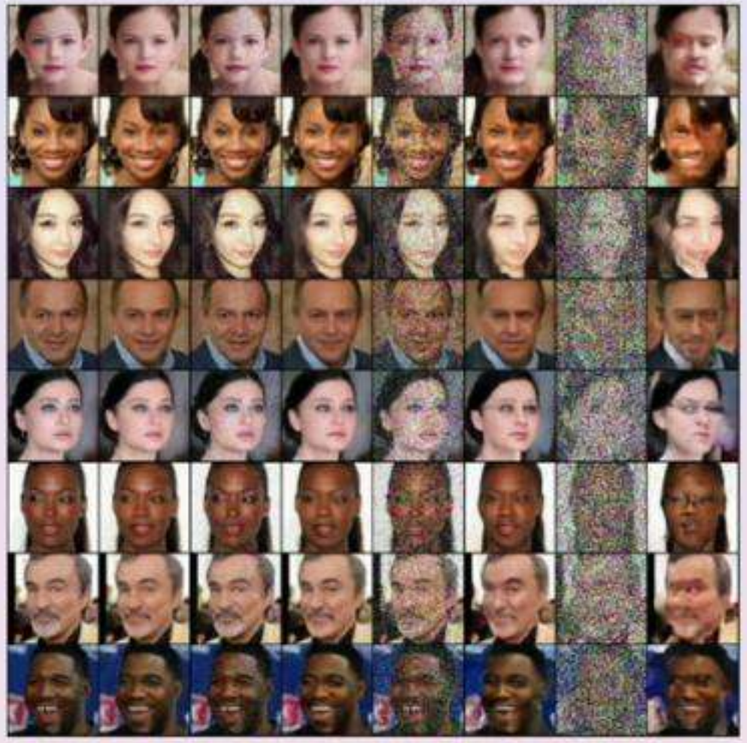

Σ is the clean facial image manifold; noisy image $\tilde{p}$ is a point close to Σ; the closest point $p \in \Sigma$ is the resulting denoised image.

Manifold view of Denoising

Traditional Method

Fourier transform the noisy image, filter out the high frequency component, inverse Fourier transform back to the denoised image.

ML Method

Use the clean facial images to train the neural network, obtain a representation of the manifold. Project the noisy image to the manifold, the projection point is the denoised image.

Key Difference

Traditional method is independent of the content of the image; ML method heavily depends on the content of the image. The prior knowledge is encoded by the manifold.

Manifold view of Denoising

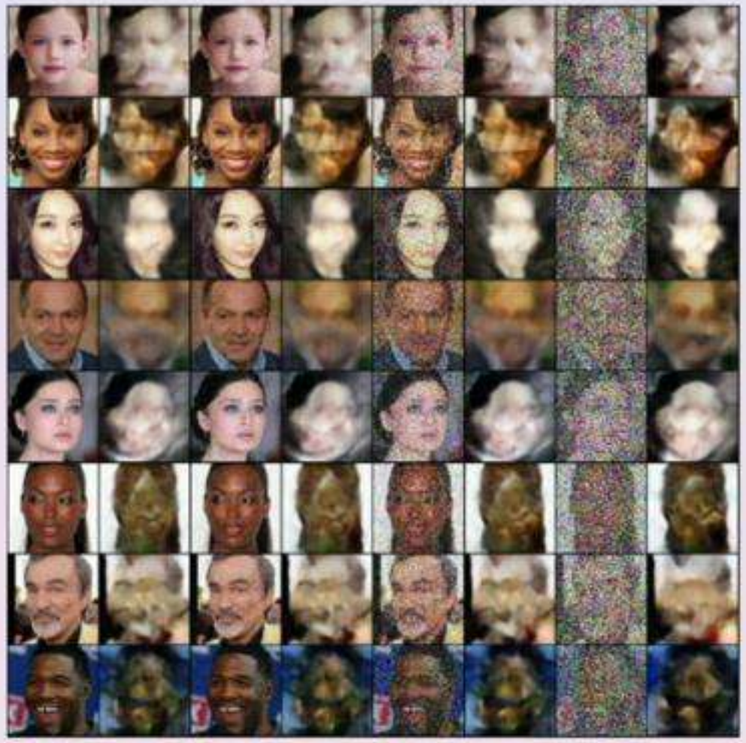

If the wrong manifold is chosen, the denoising result is of non-sense. Here we use the cat face manifold to denoise a human face image, the result looks like a cat face.

Learning Task

The central tasks for Deep Learning are

1. Learn the manifold structure from the data;
2. Represent the manifold implicitly or explicitly.

Autoencoder

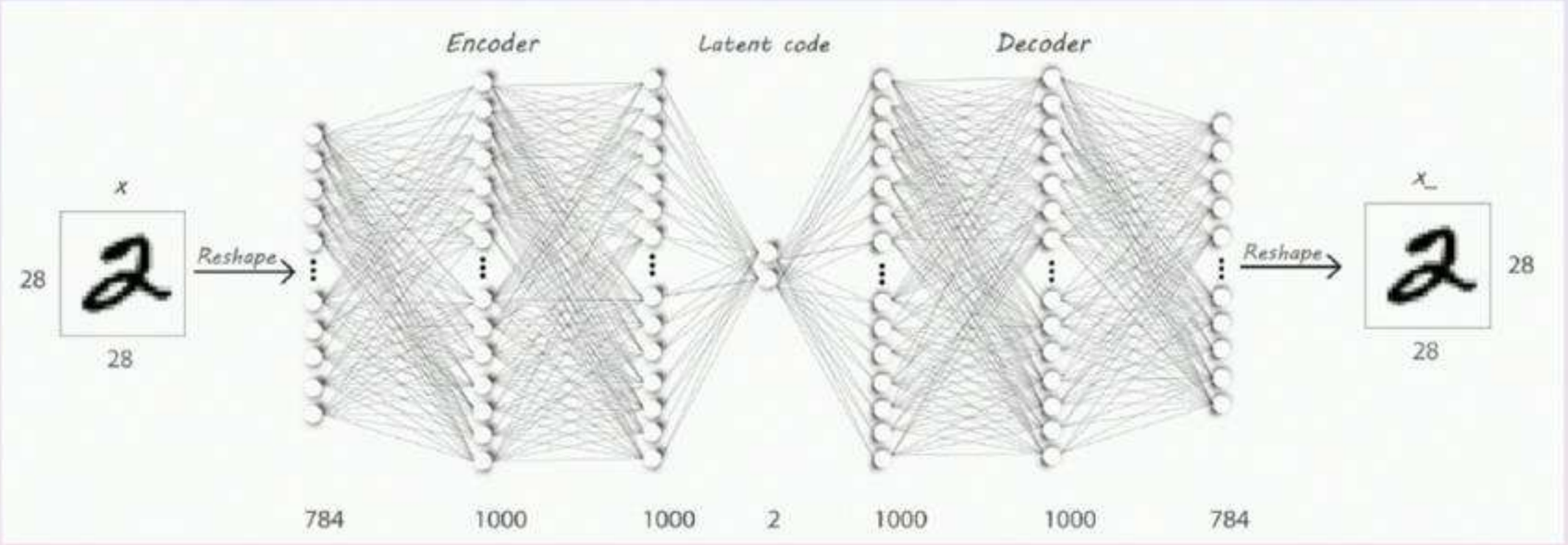

Figure: Auto-encoder architecture.

Ambient space $\mathscr{X}$, latent space $\mathscr{Z}$, encoding map $\varphi_\theta : \mathscr{X} \to \mathscr{Z}$, decoding map $\psi_\theta : \mathscr{Z} \to \mathscr{X}$.

Autoencoder

The encoder takes a sample $\mathbf{x} \in \mathscr{X}$ and maps it to $\mathbf{z} \in \mathscr{F}$, $\mathbf{z} = \varphi(\mathbf{x})$. The decoder $\psi : \mathscr{F} \to \mathscr{X}$ maps $\mathbf{z}$ to the reconstruction $\tilde{\mathbf{x}}$.

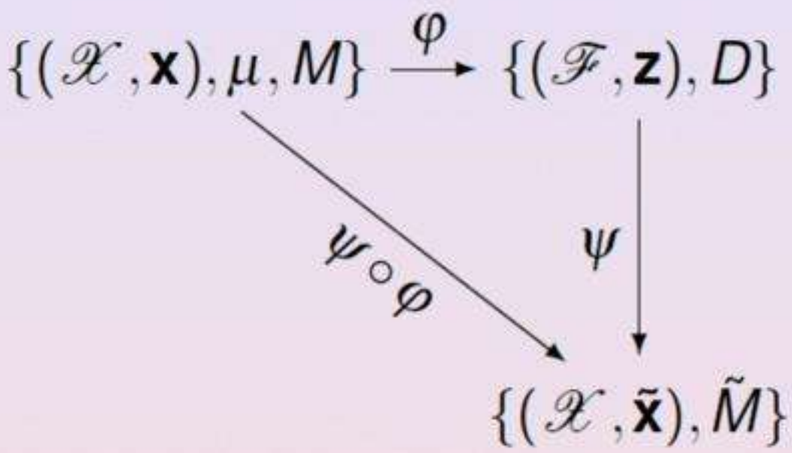

An autoencoder is trained to minimise reconstruction errors:

$$\varphi, \psi = \operatorname{argmin}_{\varphi,\psi} \int_{\mathscr{X}} \mathscr{L}(\mathbf{x}, \psi \circ \varphi(\mathbf{x})) d\mu(\mathbf{x}),$$

where $\mathscr{L}(\cdot,\cdot)$ is the loss function, such as squared errors. The reconstructed manifold $\tilde{M} = \psi \circ \varphi(M)$ is used as an approximation of M.

ReLU DNN

Definition (ReLU DNN)

For any number of hidden layers $k \in \mathbb{N}$, input and output dimensions $w_0, w_{k+1} \in \mathbb{N}$, a $\mathbb{R}^{w_0} \to \mathbb{R}^{w_{k+1}}$ ReLU DNN is given by specifying a sequence of k natural numbers $w_1, w_2, \ldots, w_k$ representing widths of the hidden layers, a set of k affine transformations $T_i : \mathbb{R}^{w_{i-1}} \to \mathbb{R}^{w_i}$ for $i = 1, \ldots, k$ and a linear transformation $T_{k+1} : \mathbb{R}^{w_k} \to \mathbb{R}^{w_{k+1}}$ corresponding to weights of hidden layers.

The mapping $\varphi_\theta : \mathbb{R}^{w_0} \to \mathbb{R}^{w_{k+1}}$ represented by this ReLU DNN is

$$\varphi = T_{k+1} \circ \sigma \circ T_k \circ \cdots \circ T_2 \circ \sigma \circ T_1, \tag{1}$$

where $\circ$ denotes mapping composition, θ represent all the weight and bias parameters.

Activated Path

Fix the encoding map φ_θ , let the set of all neurons in the network is denoted as $\mathscr{S}$, all the subsets is denoted as $2^{\mathscr{S}}$.

Definition (Activated Path)

Given a point $\mathbf{x} \in \mathscr{X}$, the *activated path* of $\mathbf{x}$ consists all the activated neurons when $\varphi_\theta(\mathbf{x})$ is evaluated, and denoted as $\rho(\mathbf{x})$. Then the activated path defines a set-valued function $\rho : \mathscr{X} \to 2^{\mathscr{S}}$.

Cell Decomposition

Definition (Cell Decomposition)

Fix a encoding map φ_θ represented by a ReLU DNN, two data points $\mathbf{x}_1, \mathbf{x}_2 \in \mathscr{X}$ are *equivalent*, denoted as $\mathbf{x}_1 \sim \mathbf{x}_2$, if they share the same activated path, $\rho(\mathbf{x}_1) = \rho(\mathbf{x}_2)$. Then each equivalence relation partitions the ambient space $\mathscr{X}$ into cells,

$$\mathscr{D}(\varphi_\theta) : \mathscr{X} = \bigcup_\alpha U_\alpha,$$

each equivalence class corresponds to a cell: $\mathbf{x}_1, \mathbf{x}_2 \in U_\alpha$ if and only if $\mathbf{x}_1 \sim \mathbf{x}_2$. $\mathscr{D}(\varphi_\theta)$ is called the cell decomposition induced by the encoding map φ_θ.

Furthermore, φ_θ maps the cell decomposition in the ambient space $\mathscr{D}(\varphi_\theta)$ to a cell decomposition in the latent space.

Encoding/Decoding

a. Input manifold $M \subset \mathscr{X}$ b. latent representation $D = \varphi_\theta(M) \subset \mathscr{Z}$ c. reconstructed mfld $\tilde{M} = \psi_\theta(D) \subset \mathscr{X}$

Figure: Auto-encoder pipeline.

Piecewise Linear Mapping

d. cell decomposition $\mathscr{D}(\varphi_\theta)$

e. latent space cell decomposition

f. cell decomposition $\mathscr{D}(\psi_\theta \circ \varphi_\theta)$

Piecewise linear encoding/decoding maps induce cell decompositions of the ambient space and the latent space.

RL Complexity of a DNN

Definition (Rectified Linear Complexity of a ReLU DNN)

Given a ReLU DNN $N(w_0, \ldots, w_{k+1})$, its rectified linear complexity is the upper bound of the number of pieces of all PL functions φ_θ represented by N,

$$\mathcal{N}(N) := \max_\theta \mathcal{N}(\varphi_\theta),$$

where $\mathcal{N}(\varphi_\theta)$ is the number of pieces of the PL function φ_θ.

Rectified Linear complexity gives a measurement for the representation capability of a neural network.

RL Complexity Estimate

Lemma

The maximum number of parts one can get when cutting d-dimensional space $\mathbb{R}^d$ with n hyperplanes is denoted as $\mathscr{C}(d,n)$, then

$$\mathscr{C}(d,n) = \binom{n}{0} + \binom{n}{1} + \binom{n}{2} + \cdots + \binom{n}{d}. \tag{2}$$

Proof.

Suppose n hyperplanes cut $\mathbb{R}^d$ into $\mathscr{C}(d,n)$ cells, each cell is a convex polyhedron. The $(n+1)$-th hyperplane is π, then the first n hyperplanes intersection π and partition π into $\mathscr{C}(d-1,n)$ cells, each cell on π partitions a polyhedron in $\mathbb{R}^d$ into 2 cells, hence we get the formula

$$\mathscr{C}(d,n+1) = \mathscr{C}(d,n) + \mathscr{C}(d-1,n).$$

RL Complexity Upper Bound

Theorem (Rectified Linear Complexity of a ReLU DNN)

Given a ReLU DNN $N(w_0, \ldots, w_{k+1})$, representing PL mappings $\varphi_\theta : \mathbb{R}^{w_0} \to \mathbb{R}^{w_{k+1}}$ with k hidden layers of widths $\{w_i\}_{i=1}^{k}$, then the linear rectified complexity of N has an upper bound,

$$\mathscr{N}(N) \leq \Pi_{i=1}^{k+1} \mathscr{C}(w_{i-1}, w_i). \tag{3}$$

RL Complexity of Manifold

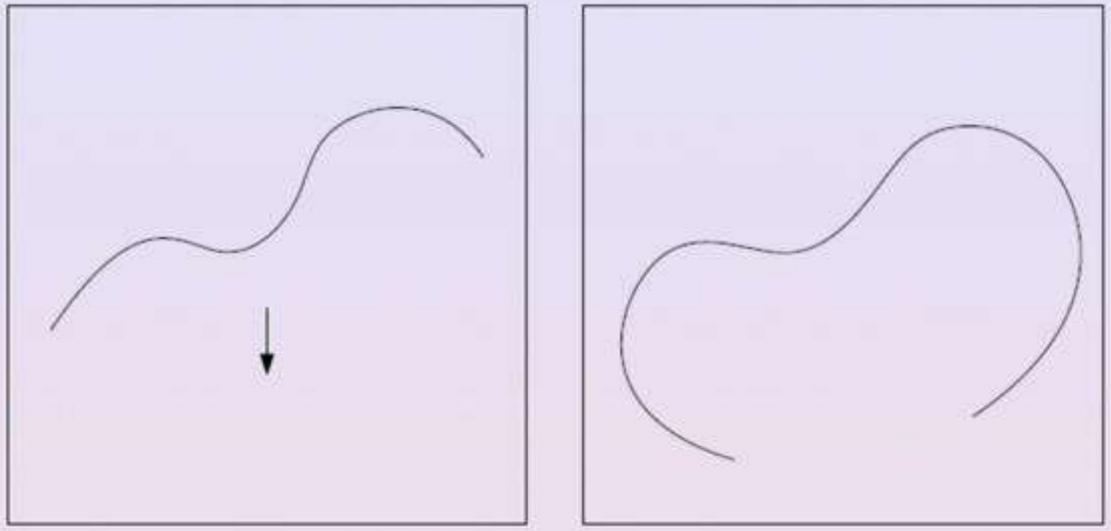

a. linear rectifiable b. non-linear-rectifiable

Definition (Linear Rectifiable Manifold)

Suppose M is a m-dimensional manifold, embedded in $\mathbb{R}^n$, we say M is linear rectifiable, if there exists an affine map $\varphi : \mathbb{R}^n \to \mathbb{R}^m$, such that the restriction of φ on M, $\varphi|_M : M \to \varphi(M) \subset \mathbb{R}^m$, is homeomorphic. φ is called the corresponding rectified linear map of M.

Manifold RL Complexity

Definition (Linear Rectifiable Atlas)

Suppose M is a m-dimensional manifold, embedded in $\mathbb{R}^n$, $\mathscr{A} = \{(U_\alpha, \varphi_\alpha\}$ is an atlas of M. If each chart $(U_\alpha, \varphi_\alpha)$ is linear rectifiable, $\varphi_\alpha : U_\alpha \to \mathbb{R}^m$ is the rectified linear map of U_α, then the atlas is called a linear rectifiable atlas of M.

Definition (Rectified Linear Complexity of a Manifold)

Suppose M is a m-dimensional manifold embedded in $\mathbb{R}^n$, the rectified linear complexity of M is denoted as $\mathscr{N}(\mathbb{R}^n, M)$ and defined as,

$$\mathscr{N}(\mathbb{R}^n, M) := \min\{|\mathscr{A}| \quad |\mathscr{A} \text{ is a linear rectifiable altas of } M\}. \tag{4}$$

Encodable Condition

Definition (Encoding Map)

Suppose M is a m-dimensional manifold, embedded in $\mathbb{R}^n$, a continuous mapping $\varphi : \mathbb{R}^n \to \mathbb{R}^m$ is called an encoding map of $(\mathbb{R}^n, M)$, if restricted on M, $\varphi|_M : M \to \varphi(M) \subset \mathbb{R}^m$ is homeomorphic.

Theorem (Encodable Condition)

Suppose a ReLU DNN $N(w_0, \ldots, w_{k+1})$ represents a PL mapping $\varphi_\theta : \mathbb{R}^n \to \mathbb{R}^m$, M is a m-dimensional manifold embedded in $\mathbb{R}^n$. If φ_θ is an encoding mapping of $(\mathbb{R}^n, M)$, then the rectified linear complexity of N is no less that the rectified linear complexity of $(\mathbb{R}^n, M)$,

$$\mathcal{N}(\mathbb{R}^n, M) \leq \mathcal{N}(\varphi_\theta) \leq \mathcal{N}(N).$$

Encodable Condition

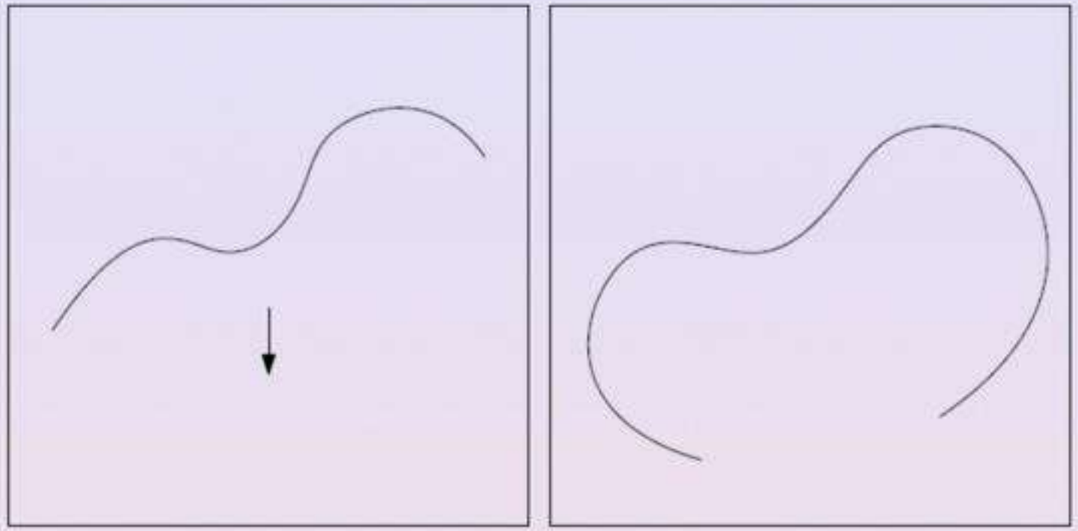

Lemma

Suppose a n dimensional manifold M is embedded in $\mathbb{R}^{n+1}$,

$$M \xrightarrow{G} \mathbb{S}^n \xrightarrow{p} \mathbb{RP}^n$$

where $G : M \to \mathbb{S}^n$ *is the Gauss map,* $\mathbb{RP}^n$ *is the real projective space, if* $p \circ G(M)$ *covers the whole* $\mathbb{RP}^n$, *then M is not linear rectifiable.*

Representation Limitation Theorem

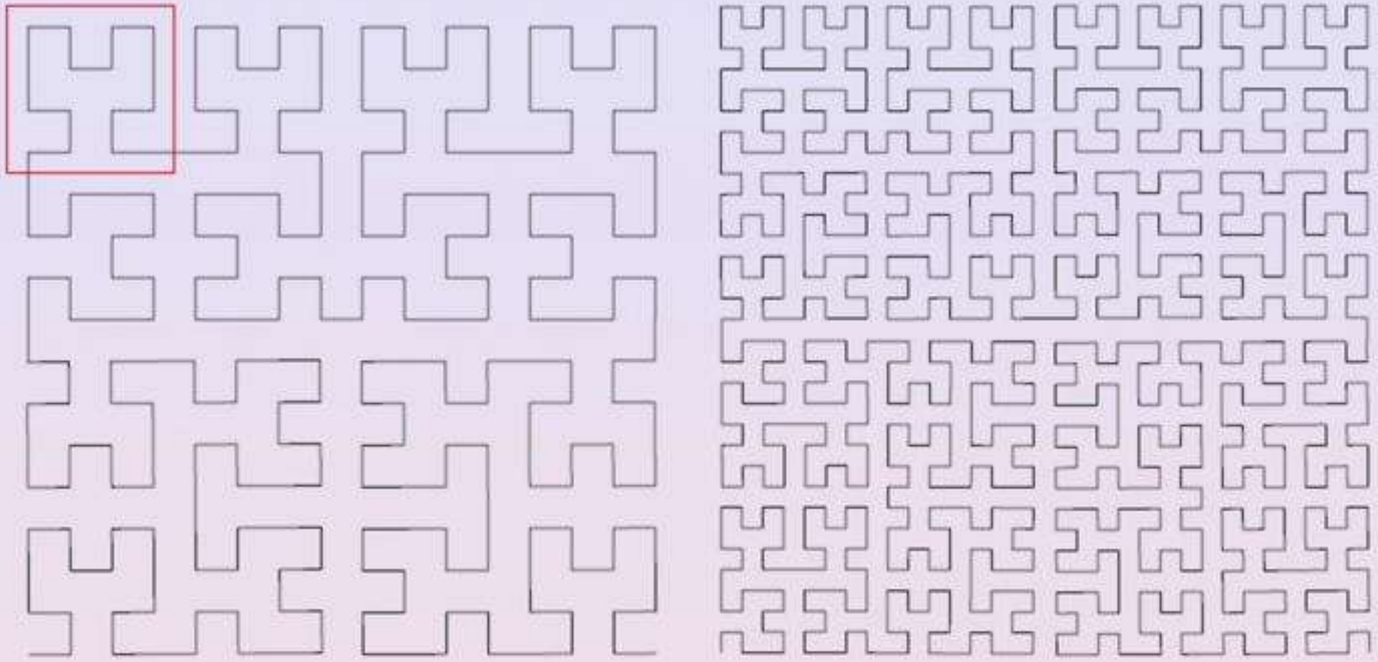

C_1 Peano curve C_2 Peano curve

Figure: $\mathcal{N}(\mathbb{R}^2, C_n) \geq 4^{n+1}$

Theorem

Given any ReLU deep neural network $N(w_0, w_1, \ldots, w_k, w_{k+1})$, there is a manifold M embedded in $\mathbb{R}^{w_0}$, such that M can not be encoded by N.

How does DL control the probability distribution?

Generative Model

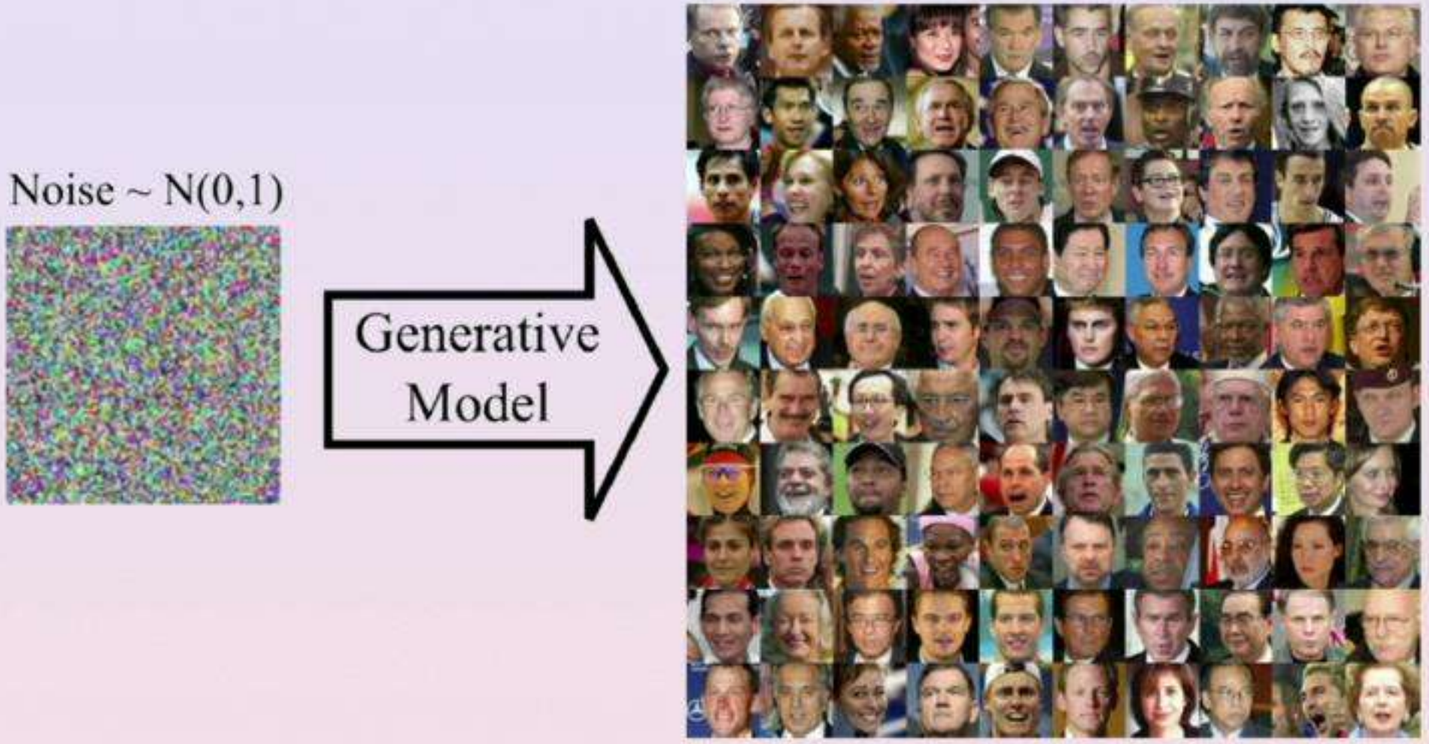

A generative model converts a white noise into a facial image.

GAN Overview

The analogy that is often used here is that the generator is like a forger trying to produce some counterfeit material, and the discriminator is like the police trying to detect the forged items.

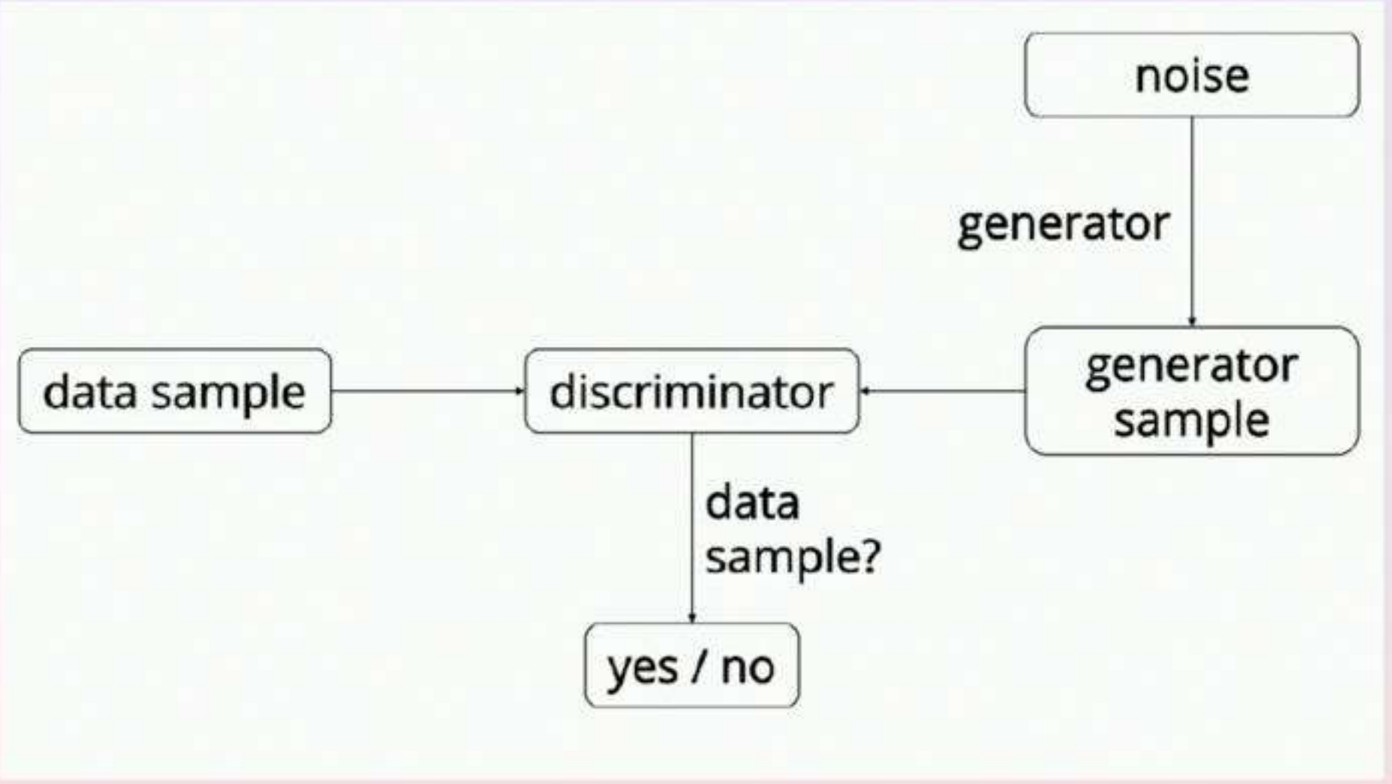

GAN Overview

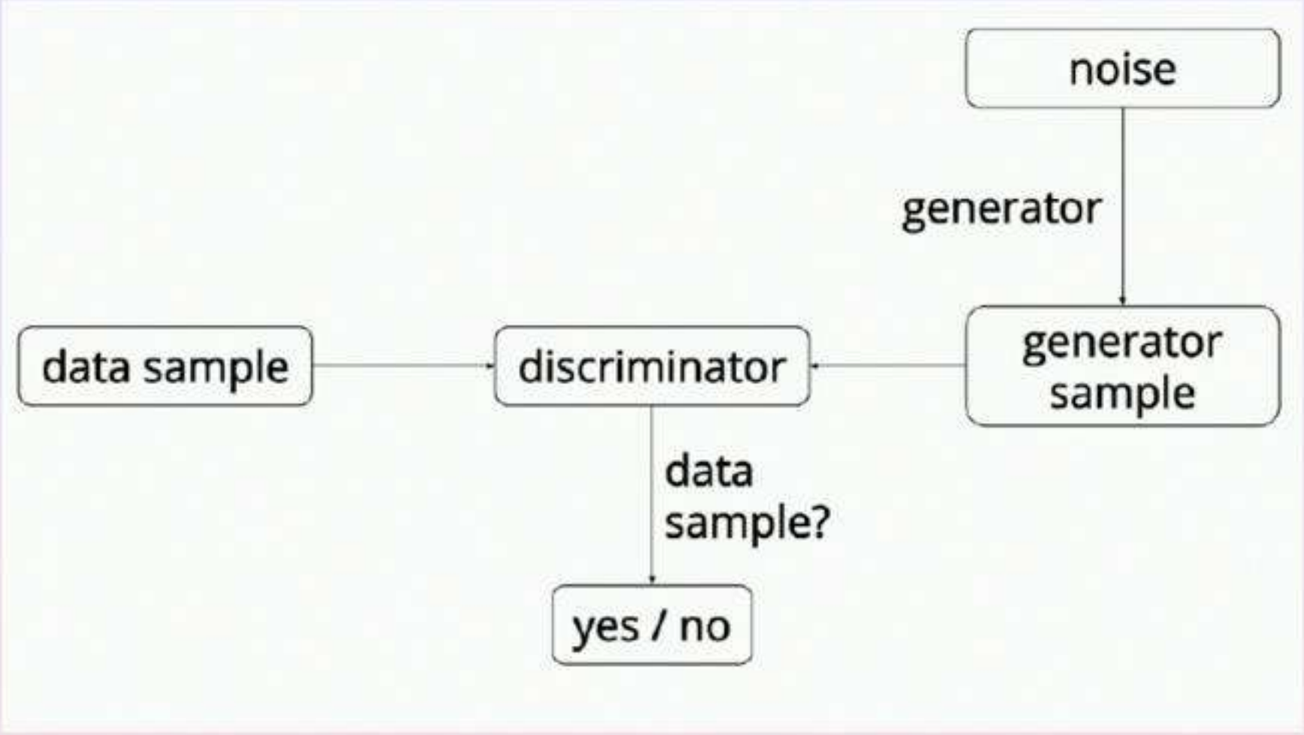

Merits

1. Automatic generate samples, the requirement for the data samples is reduced;
2. Data sample distribution can be arbitrary, without closed form expression.

GAN Overview

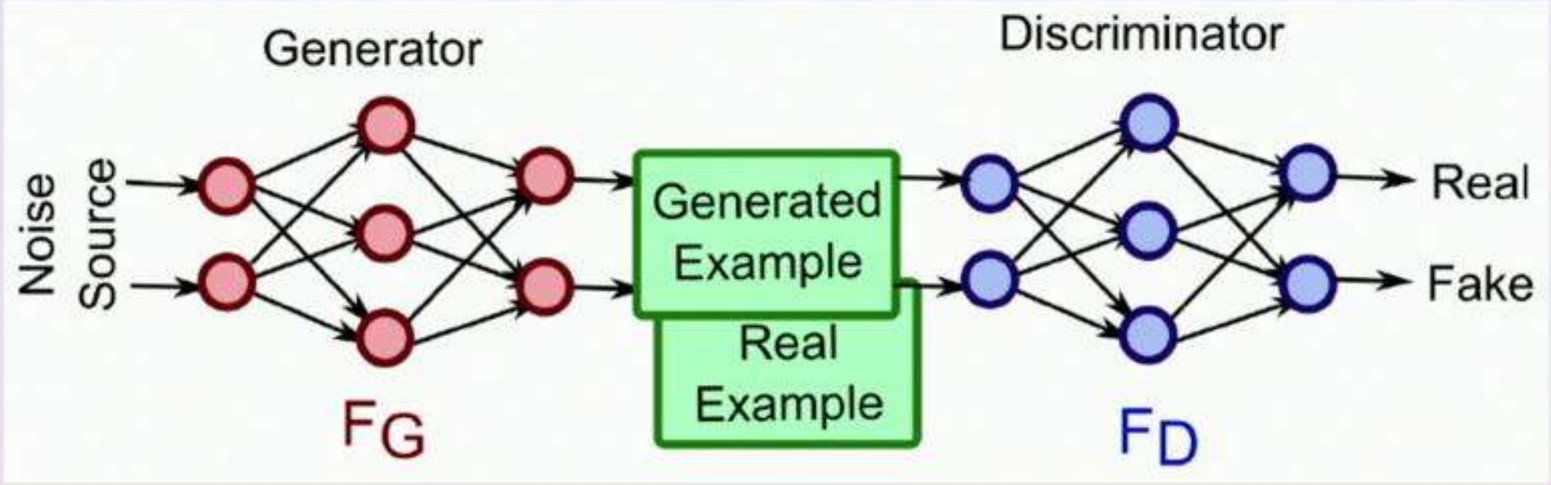

Figure: GAN DNN model.

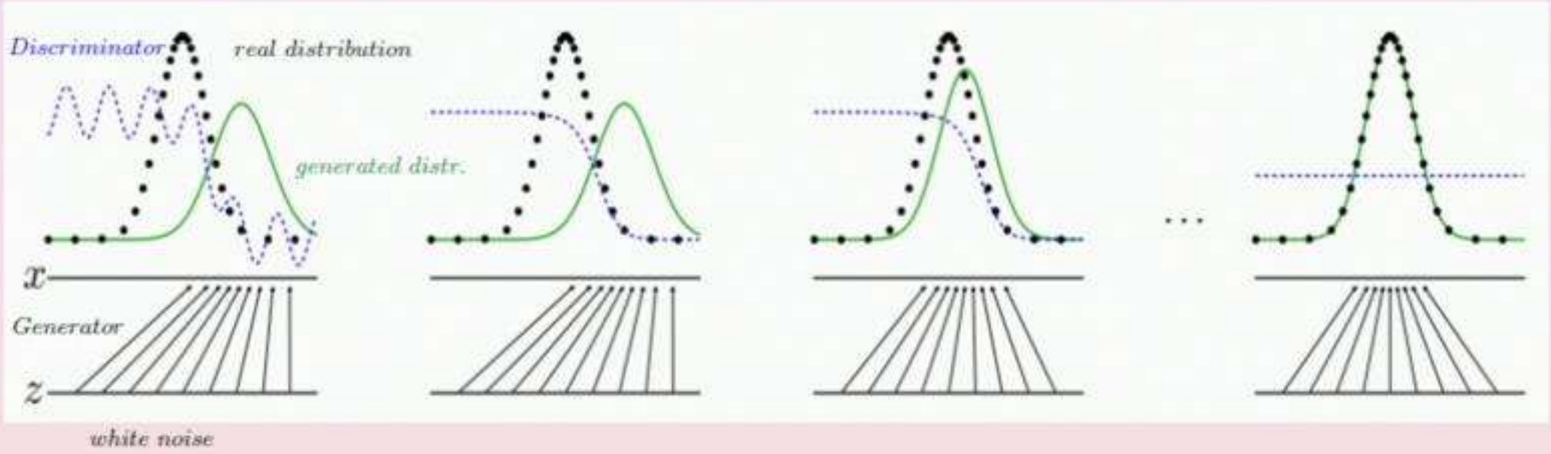

Figure: GAN learning process.

Wasserstein GAN Model

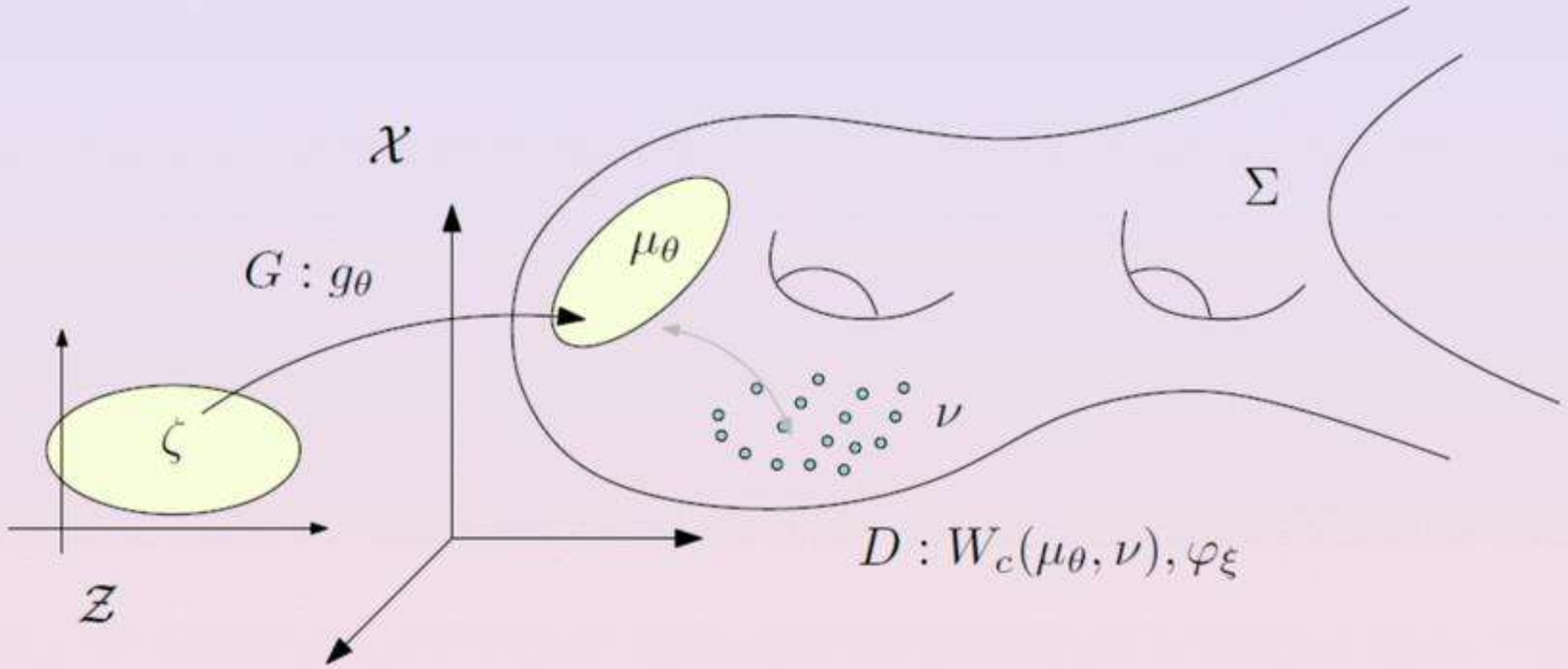

$\mathscr{X}$-image space; Σ-supporting manifold; $\mathscr{Z}$-latent space; $W_c(\cdot,\cdot)$ is the Wasserstein distance.

Wasserstein GAN Model

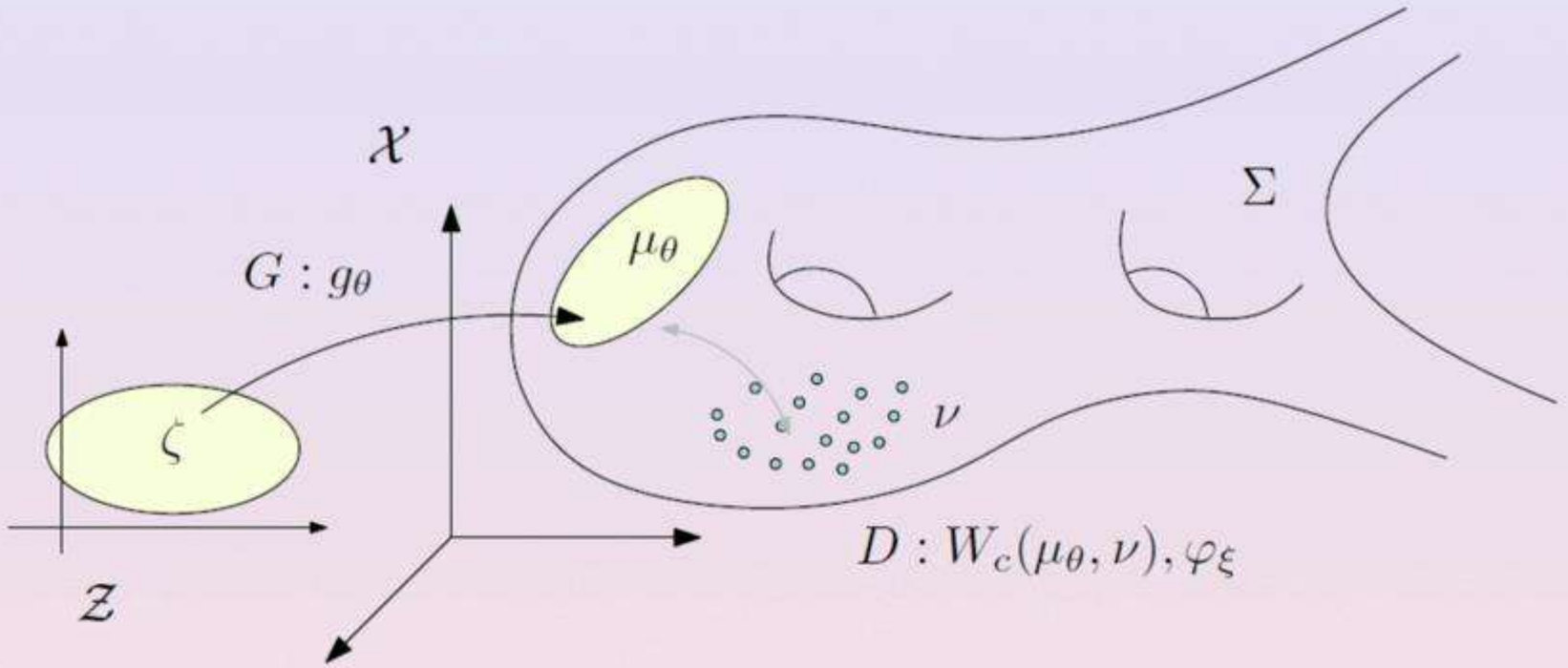

ν-training data distribution; ζ-uniform distribution;
$\mu_\theta = g_{\theta\#}\zeta$-generated distribution; G - generator computes g_θ;
D -discriminator, measures the Wasserstein distance between
ν and μ_θ, $W_c(\mu_\theta, \nu)$.

Generative Model

Generative Model

$G : \mathscr{Z} \to \mathscr{X}$ maps a fixed probability distribution ζ to the training data probability distribution ν.

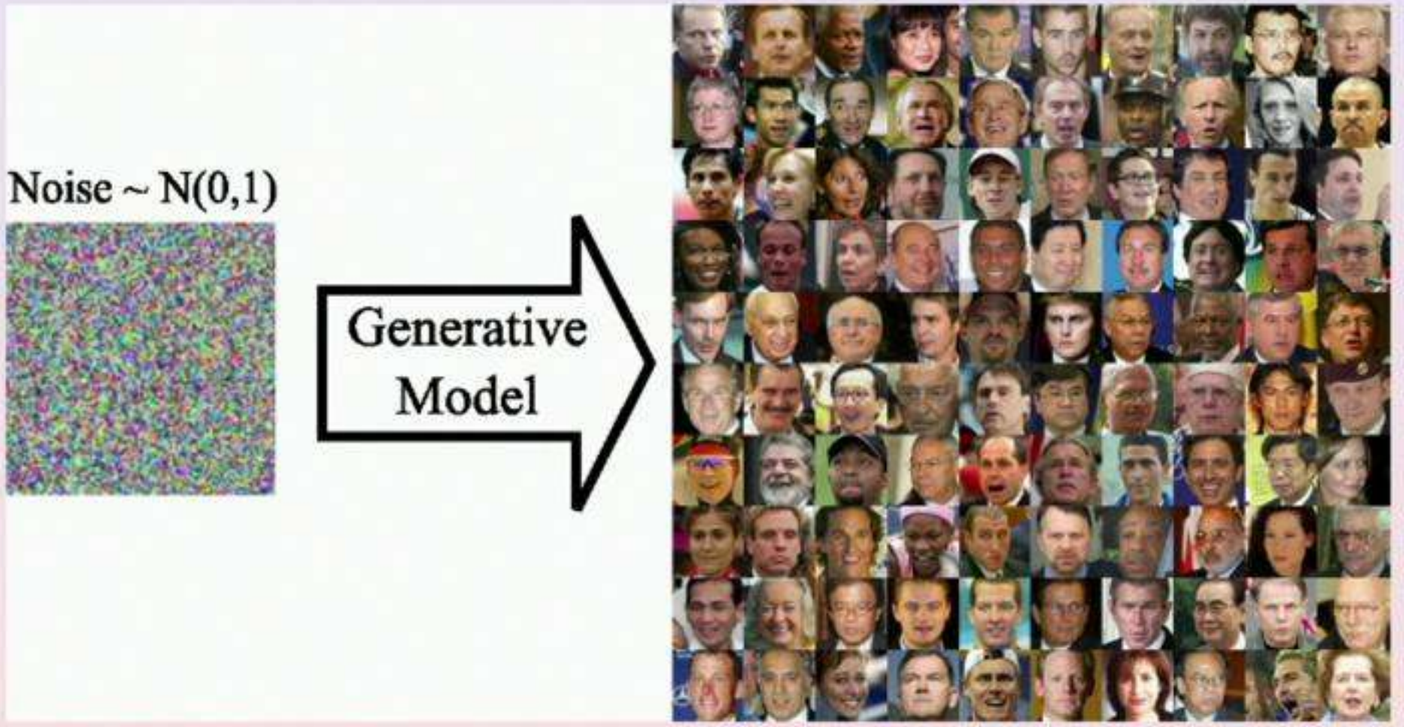

Overview

Wasserstein Space

Given a Riemannian manifold M, all the probability distributions on M form an infinite dimensional manifold Wasserstein space $\mathscr{W}(M)$, the distance between two probability distributions is given by the so-called Wasserstein distance.

Optimal Mass Transportation

Given two probability measures $\mu, \nu \in \mathscr{W}(M)$, there is a unique optimal mass transportation map $T : M \to M$, φ maps μ to ν with the minimal transportation cost. The transportation cost of the optimal transportation map is the Wasserstein distance between μ and ν.

Optimal Mass Transportation

Definition (Measure-Preserving Mapping)

Given two bounded domains in $\mathbb{R}^n$ with probability measures (X, μ) and (Y, ν), with equal total measure $\mu(X) = \nu(Y)$, a transportation mapping $T : X \to Y$ is measure-preserving, if for any measurable set $B \subset Y$,

$$\int_{T^{-1}(B)} d\mu(x) = \int_B d\nu(y),$$

and denoted as $T_{\#}\mu = \nu$.

Suppose T is a smooth map, then measure-preserving condition is equivalent to the Jacobian equation $\mu(x)dx = \nu(y)dy$

$$det(DT) = \frac{\mu(x)}{\nu \circ T(x)}.$$

Optimal Mass Transportation

Definition (Transportation Cost)

Suppose the cost of moving a unit mass from point x to point y is $c(x, y)$, for a transportation map $T : (X, \mu) \to (Y, \nu)$, the total transportation cost is

$$\mathscr{C}(T) = \int_X c(\mathbf{x}, T(\mathbf{x}))d\mu(\mathbf{x}).$$

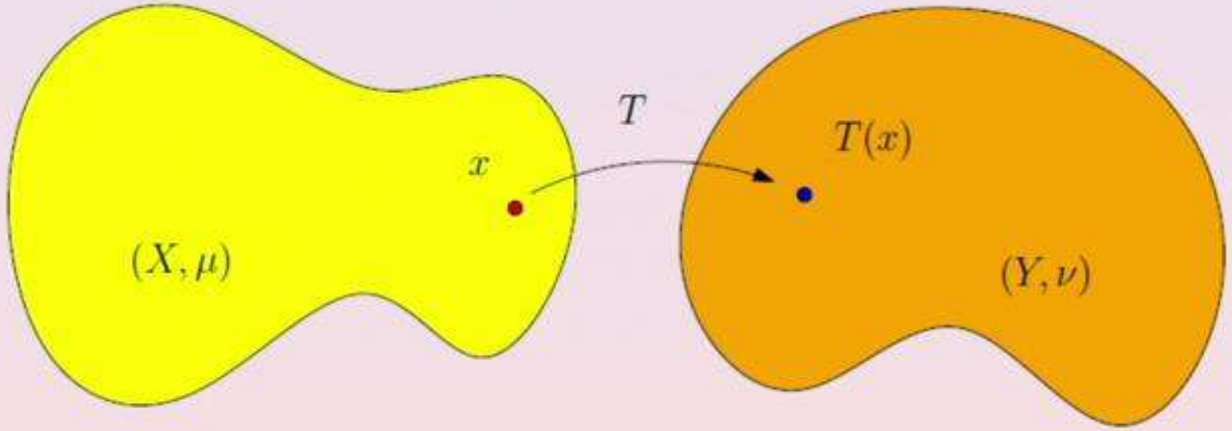

Cost Function $c(x,y)$

The cost of moving a unit mass from point x to point y.

$$Monge(1781): c(x,y) = |x-y|.$$

This is the natural cost function. Other cost functions include

$$\begin{aligned} c(x,y) &= |x-y|^p, p \neq 0 \\ c(x,y) &= -\log|x-y| \\ c(x,y) &= \sqrt{\varepsilon^2 + |x-y|^2}, \varepsilon > 0 \end{aligned}$$

Any function can be cost function. It can be negative.

Monge Problem

Problem (Monge)

Find a measure-preserving transportation map $T : (X, \mu) \to (Y, \mu)$ that minimizes the transportation cost,

$$(MP) \qquad \min_{T_{\#}\mu=\nu} \mathscr{C}(T) = \min_{T_{\#}\mu=\nu} \int_X c(x, T(x)) d\mu(x).$$

such kind of map is called the optimal mass transportation map.

Definition (Wasserstein distance)

The transportation cost of the optimal transportation map $T : (X, \mu) \to (Y, \nu)$ is called the Wasserstein distance between μ and ν, denoted as

$$W_c(\mu, \nu) := \min_{T_{\#}\mu=\nu} \mathscr{C}(T).$$

Kantorovich Problem

Kantorovich relaxed transportation maps to transportation schemes.

Problem (Kantorovich)

Find an optimal transportation scheme, namely a joint probability measure $\rho \in \mathscr{P}(X \times Y)$, with marginal measures $\rho_{x\#} = \mu$, $\rho_{y\#} = \nu$, that minimizes the transportation cost,

$$(KP) \qquad \min_{\rho} \left\{ \int_{X\times Y} c(x,y) d\rho(x,y) \,\middle|\, \rho_{x\#} = \mu,\ \rho_{y\#} = \nu \right\}.$$

Kantorovich solved this problem by inventing linear programming, and won Nobel's prize in economics in 1975.

Kantorovich Dual Problem

By the duality of linear programming, Kantorovich problem has the dual form:

Problem (Kantorovich Dual)

Find an functions $\varphi : X \to \mathbb{R}$ *and* $\psi : Y \to \mathbb{R}$, *such that*

$$(DP) \quad \max_{\varphi,\psi} \left\{ \int_X \varphi(x) du(x) + \int_Y \psi(y) dv(y), \varphi(x) + \psi(y) \leq c(x,y) \right\}.$$

Kantorovich Dual Problem

Definition (c-transformation)

Given a function $\varphi : X \to \mathbb{R}$, and $c(x, y) : X \times Y \to \mathbb{R}$, its c-transform $\varphi^c : Y \to \mathbb{R}$ is given by

$$\varphi^c(y) := \inf_{x \in X} \{c(x, y) - \varphi(x)\}.$$

Problem (Kantorovich Dual)

The Kantorovich Dual problem can be reformulated as

$$(DP) \qquad \max_{\varphi} \left\{ \int_X \varphi(x) du(x) + \int_Y \varphi^c(y) dv(y) \right\}.$$

φ is called Kantorovich potential.

Brenier's Approach

Theorem (Brenier)

If $\mu, \nu > 0$ and X is convex, and the cost function is quadratic distance,

$$c(\mathbf{x}, \mathbf{y}) = \frac{1}{2}|\mathbf{x} - \mathbf{y}|^2$$

then there exists a convex function $u : X \to \mathbb{R}$ unique upto a constant, such that the unique optimal transportation map is given by the gradient map

$$T : \mathbf{x} \to \nabla u(\mathbf{x}).$$

Problem (Brenier)

Find a convex function $u : X \to \mathbb{R}$, such that

$$(BP) \qquad (\nabla u)_{\#}\mu = \nu,$$

u is called the Brenier potential.

Brenier's Approach

From Jacobian equation, one can get the necessary condition for Brenier potential.

Problem (Brenier)

Find the C^2 Brenier potential $u : X \to \mathbb{R}$ statisfies the Monge-Ampere equation

$$(BP) \qquad det\left(\frac{\partial^2 u}{\partial x_i \partial x_j}\right) = \frac{\mu(\mathbf{x})}{\nu(\nabla f(\mathbf{x}))}.$$

Brenier's Approach

Theorem (Brenier)

If $\mu, \nu > 0$ and X is convex, and the cost function is quadratic distance,

$$c(\mathbf{x}, \mathbf{y}) = \frac{1}{2}|\mathbf{x} - \mathbf{y}|^2$$

then there exists a convex function $u : X \to \mathbb{R}$ unique upto a constant, such that the unique optimal transportation map is given by the gradient map

$$T : \mathbf{x} \to \nabla u(\mathbf{x}).$$

Problem (Brenier)

Find a convex function $u : X \to \mathbb{R}$, such that

$$(BP) \qquad (\nabla u)_{\#}\mu = \nu,$$

u is called the Brenier potential.

Optimal Mass Transportation

Definition (Measure-Preserving Mapping)

Given two bounded domains in $\mathbb{R}^n$ with probability measures (X, μ) and (Y, ν), with equal total measure $\mu(X) = \nu(Y)$, a transportation mapping $T : X \to Y$ is measure-preserving, if for any measurable set $B \subset Y$,

$$\int_{T^{-1}(B)} d\mu(x) = \int_B d\nu(y),$$

and denoted as $T_{\#}\mu = \nu$.

Suppose T is a smooth map, then measure-preserving condition is equivalent to the Jacobian equation $\mu(x)dx = \nu(y)dy$

$$det(DT) = \frac{\mu(x)}{\nu \circ T(x)}.$$

Brenier's Approach

From Jacobian equation, one can get the necessary condition for Brenier potential.

Problem (Brenier)

Find the C^2 Brenier potential $u : X \to \mathbb{R}$ statisfies the Monge-Ampere equation

$$(BP) \qquad det\left(\frac{\partial^2 u}{\partial x_i \partial x_j}\right) = \frac{\mu(\mathbf{x})}{\nu(\nabla f(\mathbf{x}))}.$$

Kantorovich and Brenier potentials

Theorem

If the distance function $c(x,y) = h(x-y)$, where $h : \mathbb{R} \to \mathbb{R}$ is a strictly convex function, the Kantorovich potential $\varphi : X \to \mathbb{R}$ gives the optimal mass transportation map directly:

$$T(\mathbf{x}) = \mathbf{x} - (\nabla\varphi)^{-1}(\nabla\varphi(\mathbf{x}))$$

Corollary

Suppose $c(x,y) = \frac{1}{2}|x-y|^2$, then Kantorovich potential and Brenier potential satisfy the relation

$$u(\mathbf{x}) = \frac{1}{2}|\mathbf{x}|^2 - \varphi(\mathbf{x}).$$

Note that u is the generator, φ is the discriminator.

Convex Geometry

Kantorovich and Brenier potentials

Theorem

If the distance function $c(x,y) = h(x-y)$, where $h : \mathbb{R} \to \mathbb{R}$ is a strictly convex function, the Kantorovich potential $\varphi : X \to \mathbb{R}$ gives the optimal mass transportation map directly:

$$T(\mathbf{x}) = \mathbf{x} - (\nabla\varphi)^{-1}(\nabla\varphi(\mathbf{x}))$$

Corollary

Suppose $c(x,y) = \frac{1}{2}|x-y|^2$, then Kantorovich potential and Brenier potential satisfy the relation

$$u(\mathbf{x}) = \frac{1}{2}|\mathbf{x}|^2 - \varphi(\mathbf{x}).$$

Note that u is the generator, φ is the discriminator.

Brenier's Approach

From Jacobian equation, one can get the necessary condition for Brenier potential.

Problem (Brenier)

Find the C^2 Brenier potential $u : X \to \mathbb{R}$ statisfies the Monge-Ampere equation

$$(BP) \qquad det\left(\frac{\partial^2 u}{\partial x_i \partial x_j}\right) = \frac{\mu(\mathbf{x})}{\nu(\nabla f(\mathbf{x}))}.$$

Minkowski problem - 2D Case

Example

A convex polygon P in $\mathbb{R}^2$ is determined by its edge lengths A_i and the unit normal vectors $\mathbf{n}_i$.

Take any $\mathbf{u} \in \mathbb{R}^2$ and project P to $\mathbf{u}$, then $\langle \sum_i A_i \mathbf{n}_i, \mathbf{u} \rangle = \mathbf{0}$, therefore

$$\sum_i A_i \mathbf{n}_i = \mathbf{0}.$$

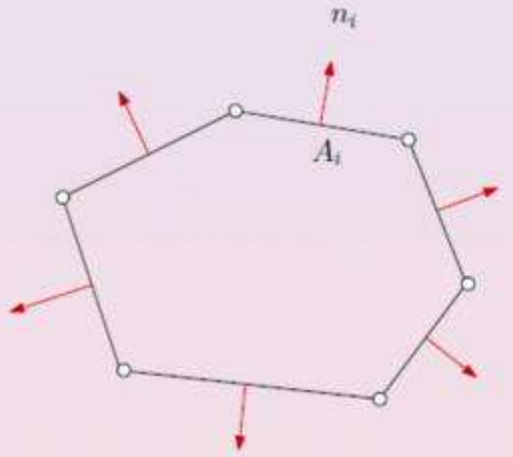

Minkowski problem - General Case

Minkowski Problem

Given k unit vectors $\mathbf{n}_1, \cdots, \mathbf{n}_k$ not contained in a half-space in $\mathbb{R}^n$ and $A_1, \cdots, A_k > 0$, such that

$$\sum_i A_i \mathbf{n}_i = \mathbf{0},$$

find a compact convex polytope P with exactly k codimension-1 faces $F_1, \cdots, F_k$, such that

1. $area(F_i) = A_i$,
2. $\mathbf{n}_i \perp F_i$.

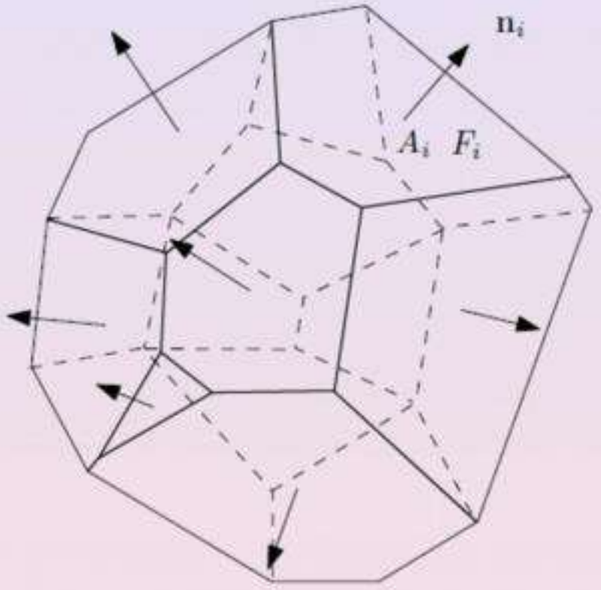

Minkowski problem - General Case

Theorem (Minkowski)

P exists and is unique up to translations.

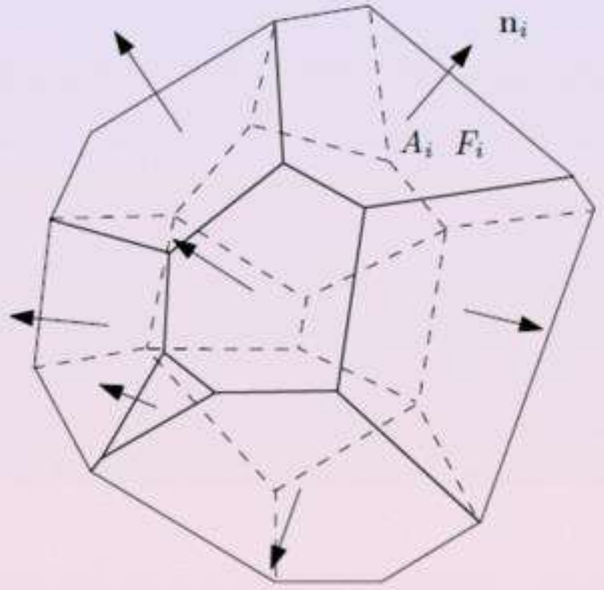

Brunn-Minkowski inequality

Theorem (Brunn-Minkowski)

For every pair of nonempty compact subsets A and B of $\mathbb{R}^n$ and every $0 \leq t \leq 1$,

$$[Vol(tA \oplus (1-t)B)]^{\frac{1}{n}} \geq t[vol(A)]^{\frac{1}{n}} + (1-t)[vol(B)]^{\frac{1}{n}}.$$

For convex sets A and B, the inequality is strick for $0 < t < 1$ unless A and B are homothetic i.e. are equal up to translation and dilation.

Alexandrov Theorem

Theorem (Alexandrov 1950)

Given Ω compact convex domain in $\mathbb{R}^n$, $p_1, \cdots, p_k$ distinct in $\mathbb{R}^n$, $A_1, \cdots, A_k > 0$, such that $\sum A_i = Vol(\Omega)$, there exists PL convex function

$$f(\mathbf{x}) := \max\{\langle \mathbf{x}, \mathbf{p}_i \rangle + h_i | i = 1, \cdots, k\}$$

unique up to translation such that

$$Vol(W_i) = Vol(\{\mathbf{x} | \nabla f(\mathbf{x}) = \mathbf{p}_i\}) = A_i.$$

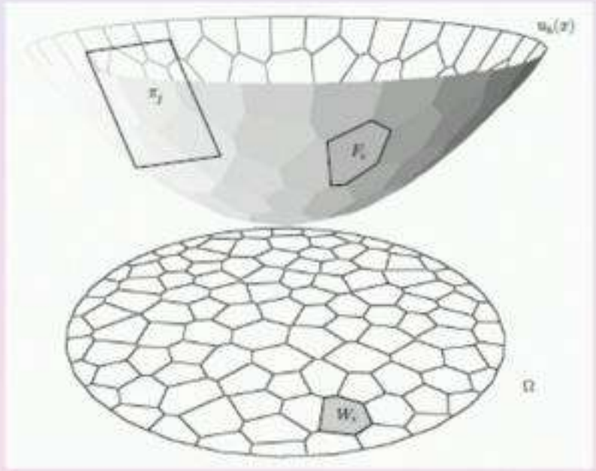

Alexandrov's proof is topological, not variational. It has been open for years to find a constructive proof.

Variational Proof

Theorem (Gu-Luo-Sun-Yau 2013)

Ω is a compact convex domain in $\mathbb{R}^n$, $y_1, \cdots, y_k$ distinct in $\mathbb{R}^n$, μ a positive continuous measure on Ω. For any $v_1, \cdots, v_k > 0$ with $\sum v_i = \mu(\Omega)$, there exists a vector $(h_1, \cdots, h_k)$ so that

$$u(\mathbf{x}) = \max\{\langle \mathbf{x}, \mathbf{p}_i \rangle + h_i\}$$

satisfies $\mu(W_i \cap \Omega) = v_i$, where $W_i = \{\mathbf{x} | \nabla f(\mathbf{x}) = \mathbf{p}_i\}$. Furthermore, $\mathbf{h}$ is the maximum point of the convex function

$$E(\mathbf{h}) = \sum_{i=1}^{k} v_i h_i - \int_{\mathbf{0}}^{\mathbf{h}} \sum_{i=1}^{k} w_i(\eta) d\eta_i,$$

where $w_i(\eta) = \mu(W_i(\eta) \cap \Omega)$ is the μ-volume of the cell.

Variational Proof

X. Gu, F. Luo, J. Sun and S.-T. Yau, “Variational Principles for Minkowski Type Problems, Discrete Optimal Transport, and Discrete Monge-Ampere Equations”, arXiv:1302.5472

Accepted by Asian Journal of Mathematics (AJM)

Geometric Interpretation

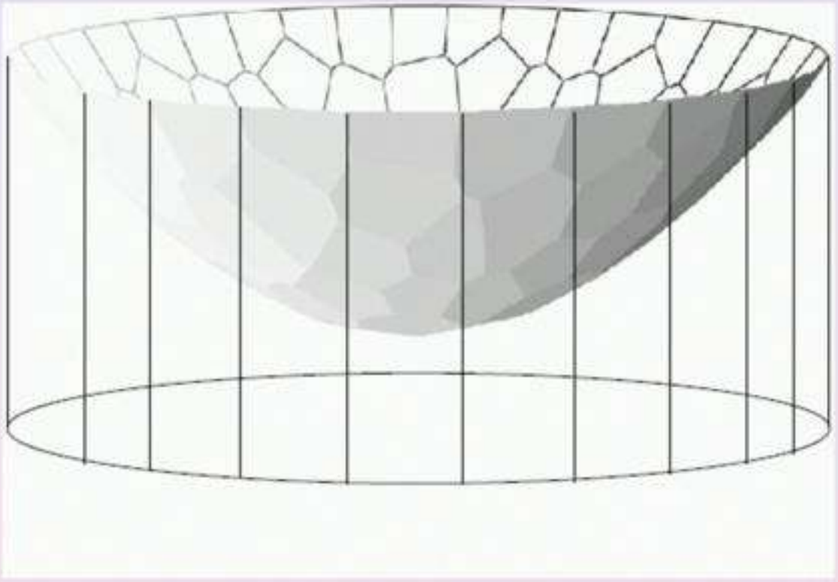

One can define a cylinder through $\partial\Omega$, the cylinder is truncated by the xy-plane and the convex polyhedron. The energy term $\int^{\mathbf{h}} \sum w_i(\eta) d\eta_i$ equals to the volume of the truncated cylinder.

Variational Proof

Theorem (Gu-Luo-Sun-Yau 2013)

Ω is a compact convex domain in $\mathbb{R}^n$, $y_1, \cdots, y_k$ distinct in $\mathbb{R}^n$, μ a positive continuous measure on Ω. For any $v_1, \cdots, v_k > 0$ with $\sum v_i = \mu(\Omega)$, there exists a vector $(h_1, \cdots, h_k)$ so that

$$u(\mathbf{x}) = \max\{\langle \mathbf{x}, \mathbf{p}_i \rangle + h_i\}$$

satisfies $\mu(W_i \cap \Omega) = v_i$, where $W_i = \{\mathbf{x} | \nabla f(\mathbf{x}) = \mathbf{p}_i\}$. Furthermore, $\mathbf{h}$ is the maximum point of the convex function

$$E(\mathbf{h}) = \sum_{i=1}^{k} v_i h_i - \int_{\mathbf{0}}^{\mathbf{h}} \sum_{i=1}^{k} w_i(\eta) d\eta_i,$$

where $w_i(\eta) = \mu(W_i(\eta) \cap \Omega)$ is the μ-volume of the cell.

Geometric Interpretation

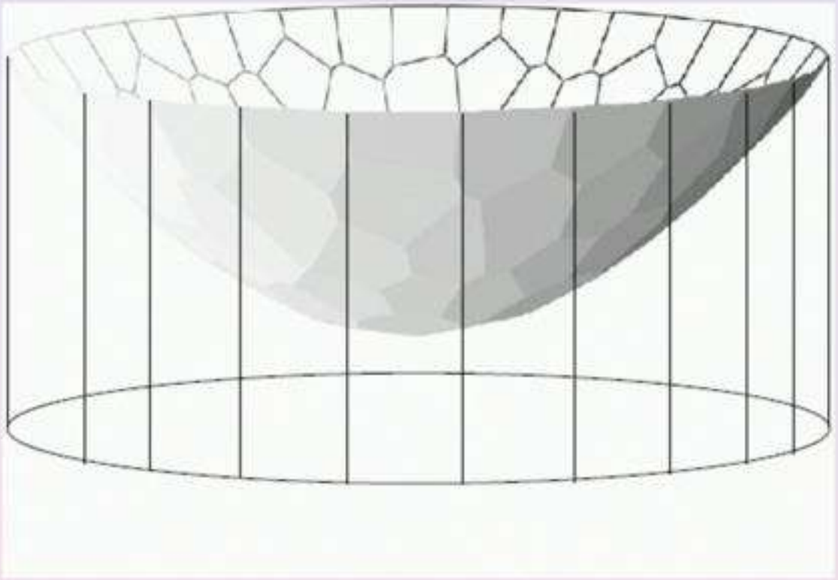

One can define a cylinder through $\partial\Omega$, the cylinder is truncated by the xy-plane and the convex polyhedron. The energy term $\int^{\mathbf{h}} \sum w_i(\eta) d\eta_i$ equals to the volume of the truncated cylinder.

Computational Algorithm

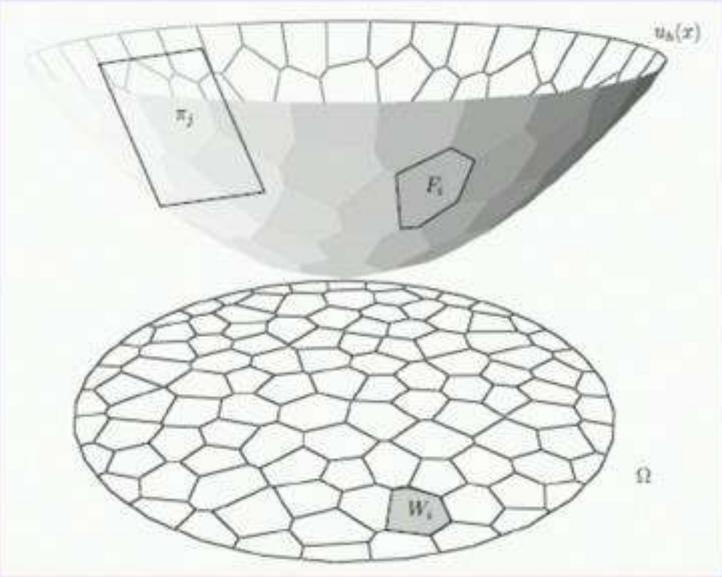

Definition (Alexandrov Potential)

The concave energy is

$$E(h_1, h_2, \cdots, h_k) = \sum_{i=1}^{k} \nu_i h_i - \int_{\mathbf{0}}^{\mathbf{h}} \sum_{j=1}^{k} w_j(\eta) d\eta_j,$$

Geometrically, the energy is the volume beneath the parabola.

Computational Algorithm

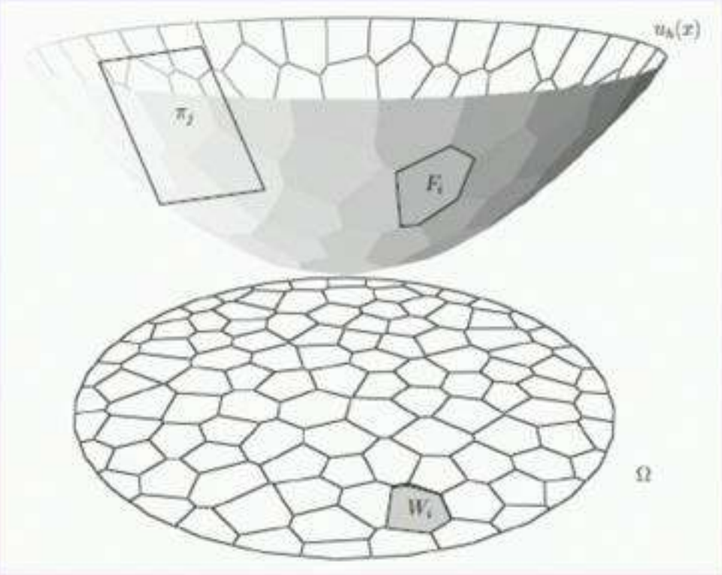

The gradient of the Alexanrov potential is the differences between the target measure and the current measure of each cell

$$\nabla E(h_1, h_2, \cdots, h_k) = (\nu_1 - w_1, \nu_2 - w_2, \cdots, \nu_k - w_k)$$

Computational Algorithm

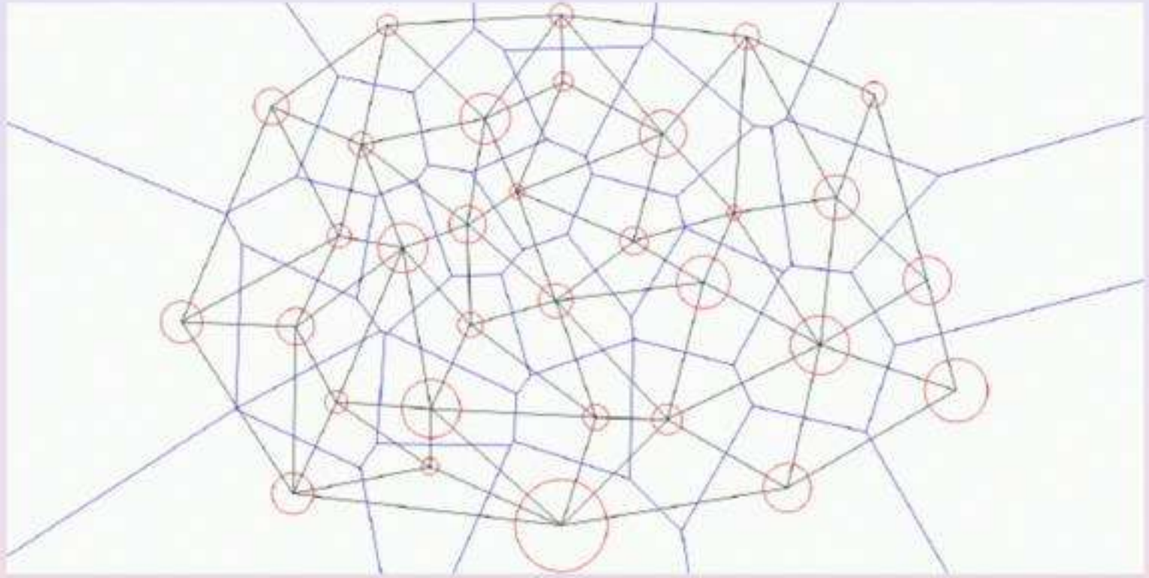

The Hessian of the energy is the length ratios of edge and dual edges,

$$\frac{\partial w_i}{\partial h_j} = \frac{|e_{ij}|}{|\bar{e}_{ij}|}$$

Wasserstein GAN Model

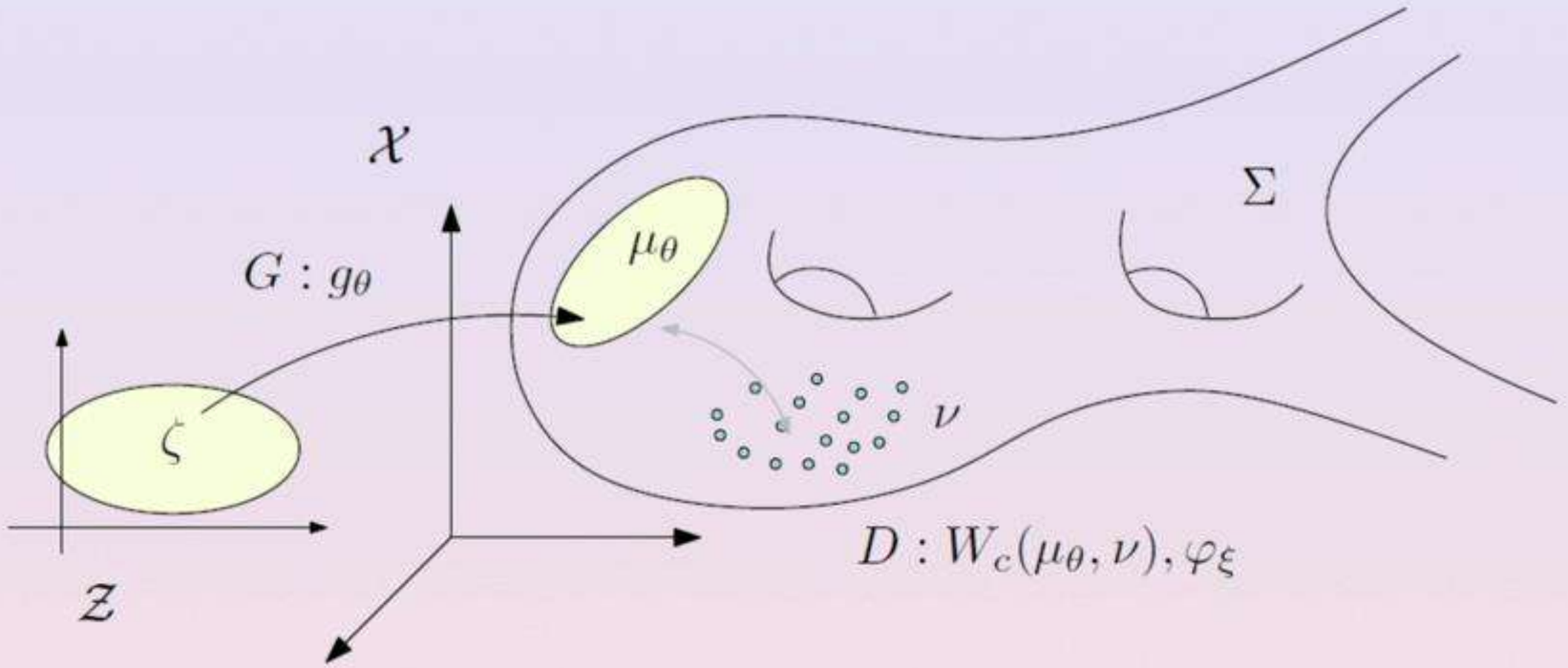

ν-training data distribution; ζ-uniform distribution;
$\mu_\theta = g_{\theta\#}\zeta$-generated distribution; G - generator computes g_θ;
D -discriminator, measures the distance between ν and μ_θ,
$W_c(\mu_\theta, \nu)$.

Computational Algorithm

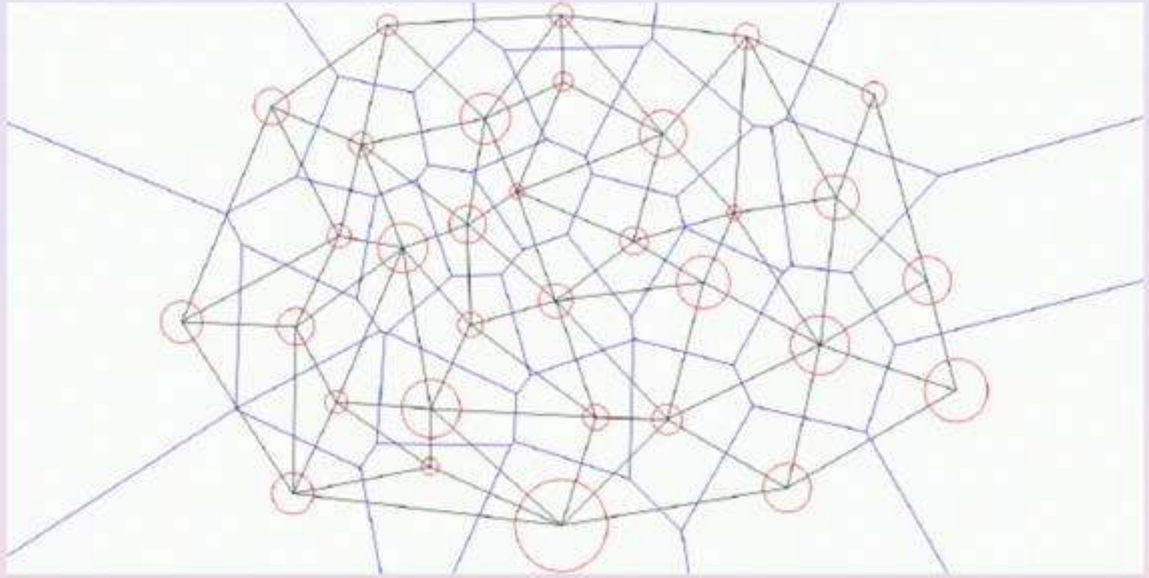

The Hessian of the energy is the length ratios of edge and dual edges,

$$\frac{\partial w_i}{\partial h_j} = \frac{|e_{ij}|}{|\bar{e}_{ij}|}$$

Wasserstein GAN Model

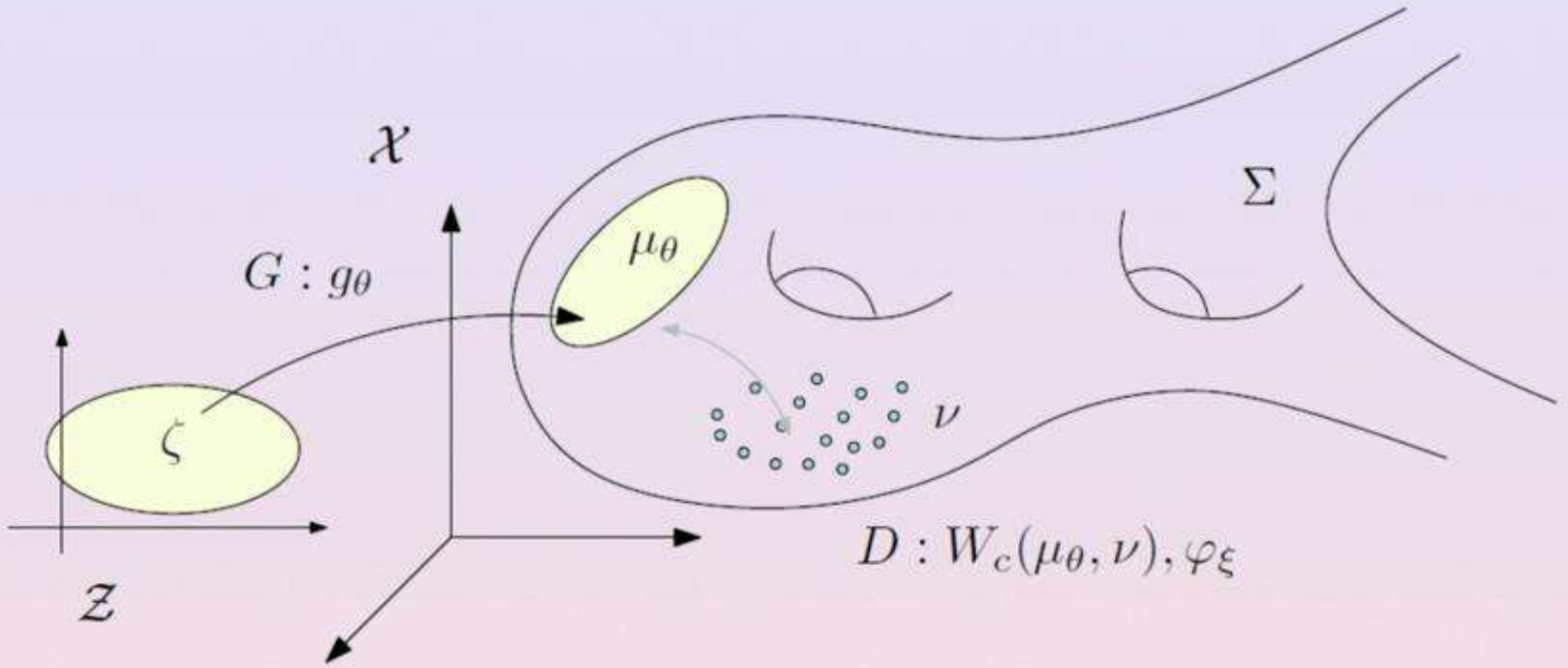

ν-training data distribution; ζ-uniform distribution;
$\mu_\theta = g_{\theta\#}\zeta$-generated distribution; G - generator computes g_θ;
D -discriminator, measures the distance between ν and μ_θ,
$W_c(\mu_\theta, \nu)$.

OMT view of WGAN

From the optimal transportation point of view, Wasserstein GAN performs the following tasks:

- The discriminator: computes the Wassersteind distance using Kantorovich Dual formula:

$$W_c(\mu_\theta, \nu) = \max_{\varphi_\xi} \int_X \varphi_\xi(x) d\mu_\theta(x) + \int_Y \varphi_\xi^c(y) d\nu(y),$$

  namely computes the Kantorovich potential φ;
- The generator: computes a measure-preserving transportation map $g_\theta : \mathcal{Z} \to \mathcal{X}$, s.t. $g_{\theta\#}\zeta = \mu_\theta = \nu$.
- The WGAN model: min-max optimization

$$\min_\theta \max_\xi \int_X \varphi_\xi \circ g_\theta(z) d\zeta(z) + \int_Y \varphi_\xi^c(y) d\nu(y)$$

OMT view of WGAN

L^1 case

When $c(x,y) = |x-y|$, $\varphi^c = -\varphi$, given φ is 1-Lipsitz, the WGAN model: min-max optimization

$$\min_{\theta}\max_{\xi}\int_X \varphi_\xi \circ g_\theta(z)d\zeta(z) - \int_Y \varphi_\xi(y)d\nu(y).$$

namely

$$\min_{\theta}\max_{\xi}\ \mathbb{E}_{z\sim\zeta}(\varphi_\xi \circ g_\theta(z)) - \mathbb{E}_{y\sim\nu}(\varphi_\xi(y)).$$

with the constraint that φ_ξ is 1-Lipsitz.

OMT view of WGAN

L^2 case

The discriminator computes the Kantorovich potential φ; the generator G computes the optimal transportation map, $T = \nabla u$, where u is the Brenier potential; The Brenier potential equals to

$$u = \frac{1}{2}|x|^2 - \varphi(x),$$

Generator G computes u, Discriminator D computes φ, hence in theory:

- G can be obtained from the optimal D without training;
- D can be obtained from the optimal G without training;
- The two deep neural networks are redundant;
- The competition between D and G is unnecessary.

Empirical Distribution

Empirical Distribution

In practice, the target probability measure is approximated by empirical distribution:

$$\nu = \sum_{i=1}^{n} \delta(y - y_i)\nu_i,$$

in general $\nu_i = 1/n$.

Semi-discrete Optimal Transportation

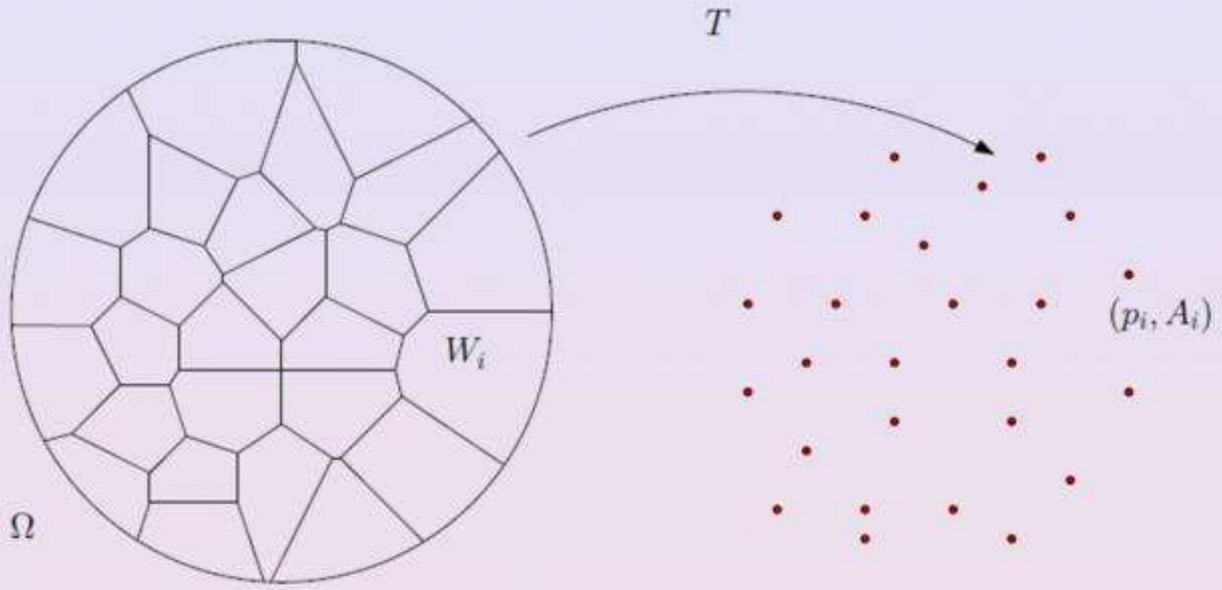

Given a compact convex domain Ω in $\mathbb{R}^n$ and $p_1, \cdots, p_k$ in $\mathbb{R}^n$ and $A_1, \cdots, A_k > 0$, find a transport map $T : U \to \{p_1, \cdots, p_k\}$ with $vol(T^{-1}(p_i)) = A_i$, so that T minimizes the transport cost

$$\frac{1}{2}\int_U |\mathbf{x} - T(\mathbf{x})|^2 d\mathbf{x}.$$

Power Diagram vs Optimal Transport Map

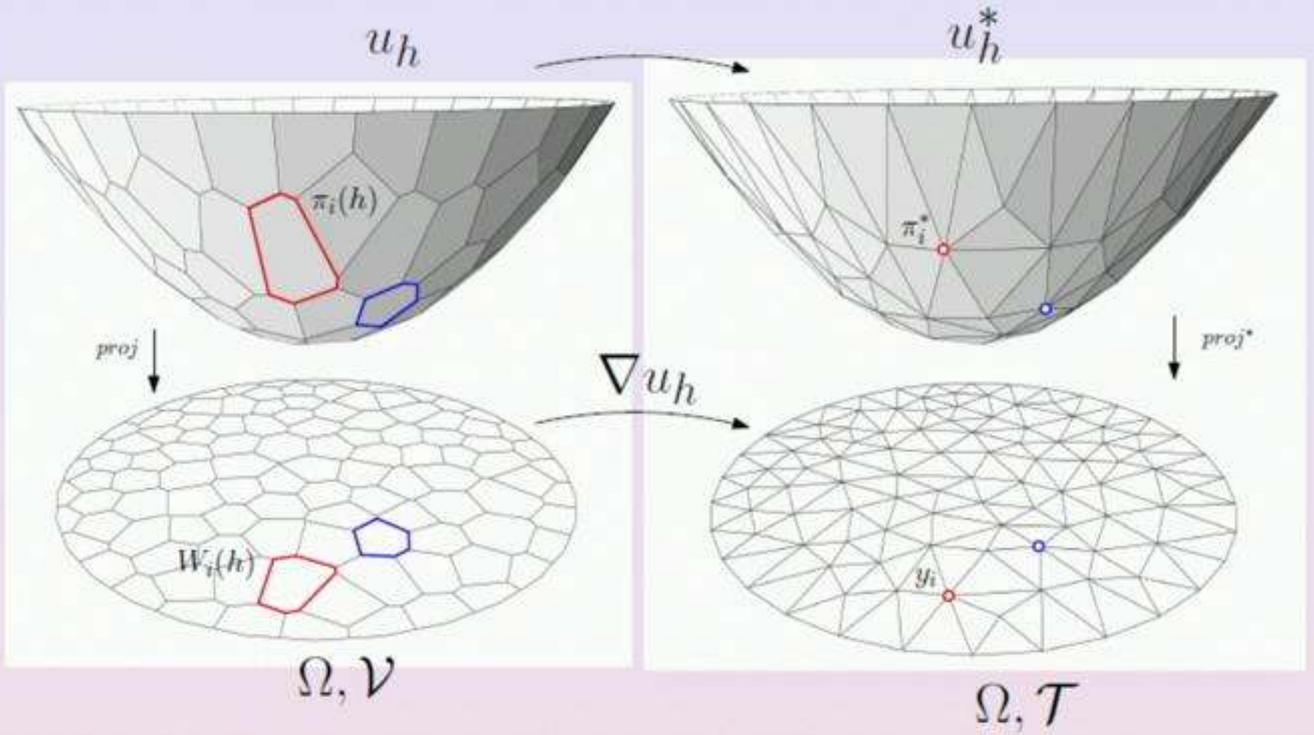

1. $\forall y_i \in Y$, construct a hyper-plane $\pi_h^i(x) = \langle x, y_i \rangle - h_i$;
2. compute the upper envelope of the planes $u_h(x) = \max_i\{\pi_h^i(x)\}$
3. produce the power diagram of Ω, $\mathcal{W}(h) = \cup_i W_i(h)$;
4. adjust the heights h, such that $\mu(W_i(h)) = \nu_i$.

Power Diagram vs Optimal Transport Map

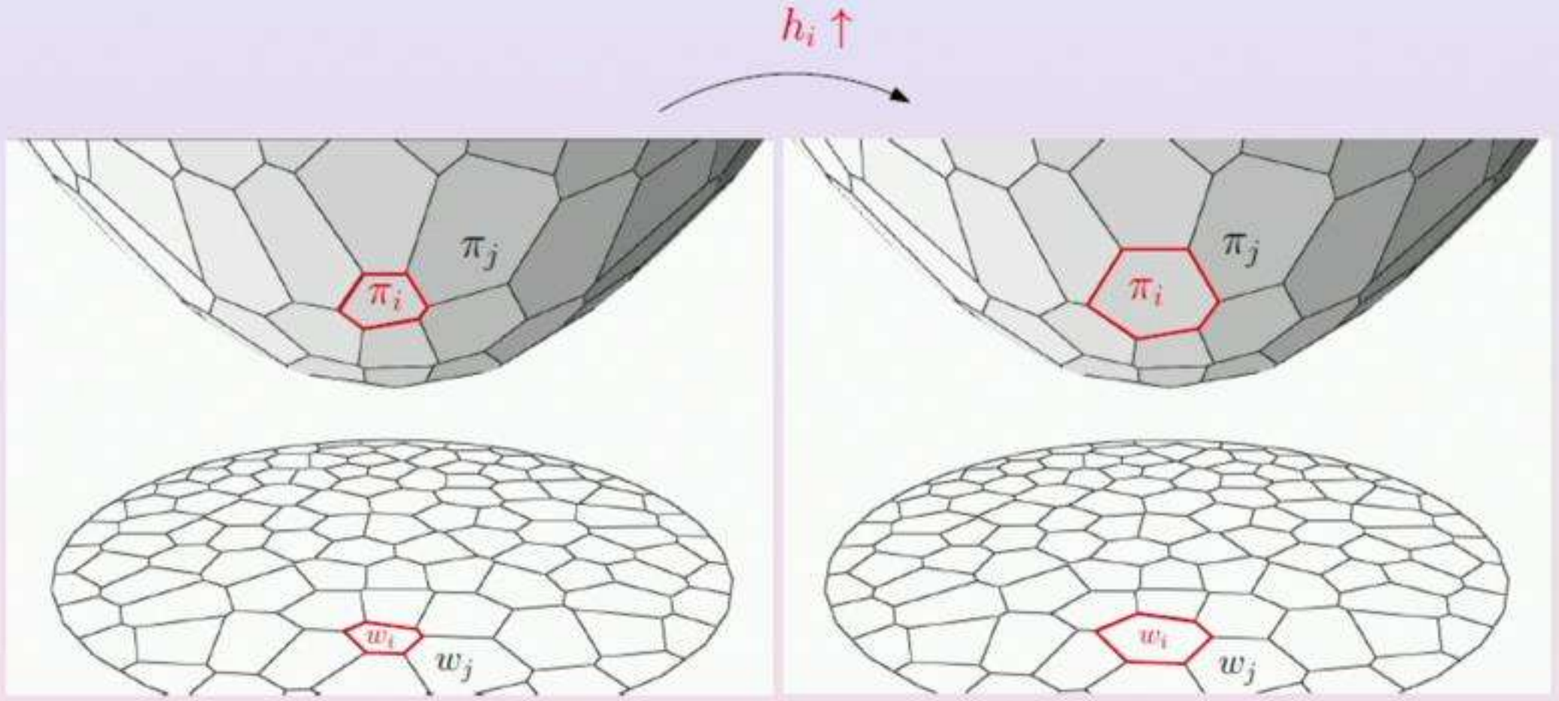

Figure: Variation of the μ-volume of top-dimensional cells.

Adjust the height of each hyper-plane, such that $\mu(W_i(h)) = \nu_i$.

Mode Collapse

Mode Collapse

- GANs are difficult to train and sensitive to hyper-parameters;
- GANs suffer from mode collapsing, the generated distributions miss some modes;
- GANs may generate unrealistic samples;

Regularity of Optimal Transportation Map

Let Ω and Ω^* be bounded domains in $\mathbb{R}^n$, let f and g be mass densities on Ω and Ω^* satisfying

1. $0 \leq f \in L^1(\Omega)$, $0 \leq g \in L^1(\Omega^*)$,

$$\int_\Omega f = \int_{\Omega^*} g.$$

2. $\exists$ constants $f_0, f_1, g_0, g_1 > 0$, such that

$$f_0 \leq f \leq f_1, g_0 \leq g \leq g_1.$$

Regularity of Optimal Transportation Map

Let (u, v) be the Kantorovich's potential functions. The optimal mapping T_u is given by

$$Du(x) = D_x c(x, T_u(x))$$

Differentiate the formula

$$D^2 u(x) = D_x^2 c(x, T_u(x)) + D_{xy}^2 c(x, T_u(x)) DT_u.$$

We obtain the equation

$$\det[D^2 u(x) - D_x^2 c(x, T_u(x))] = \det D_{xy}^2 c(x, T_u(x)) \frac{f(x)}{g(T_u(x))},$$

with the boundary condition $T_u(\Omega) = \Omega^*$.

Regularity of Optimal Transportation Map

Caffarelli obtained the regularity of optimal mappings for the cost function

$$c(x,y) = |x-y|^2$$

or equivalently $c(x,y) = x \cdot y$, then we have the standard Monge-Ampere equation

$$\det D^2 u = \frac{f(x)}{g(Du(x))},$$

with boundary condition $Du(\Omega) = \Omega^*$.

1. if $f, g > 0, \in C^\alpha$ and Ω^* is convex, then $u \in C^{2,\alpha}(\Omega)$
2. if $f, g > 0, \in C^0$ and Ω^* is convex, then $u \in W^{2,p}_{loc}(\Omega)$, $\forall p > 1$ (the continuity is needed for large p).
3. if $f, g > 0, \in C^\alpha$, both Ω and Ω^* are uniformly convex and $C^{2,\alpha}$, then $u \in C^{2,\alpha}(\bar{\Omega})$

Regularity of Optimal Transportation Map

Theorem (Ma-Trudinger-Wang)

The potential function u is C^3 smooth if the cost function c is smooth, f, g are positive, $f \in C^2(\Omega)$, $g \in C^2(\Omega^*)$, and

- *A1* $\forall x, \xi \in \mathbb{R}^n$, $\exists! y \in \mathbb{R}^n$, *s.t.* $\xi = D_x c(x, y)$ *(for existence)*
- *A2* $|D^2_{xy} c| \neq 0$.
- *A3* $\exists c_0 > 0$ *s.t.* $\forall \xi, \eta \in \mathbb{R}^n$, $\xi \perp \eta$

$$\sum (c_{ij,rs} - c^{p,q} c_{ij,p} c_{q,rs}) c^{r,k} c^{s,l} \xi_i \xi_j \eta_k \eta_l \geq c_0 |\xi|^2 |\eta|^2.$$

- *B1* Ω^* *is c-convex w.r.t.* Ω, *namely* $\forall x_0 \in \Omega$,

$$\Omega^*_{x_0} := D_x c(x_0, \Omega^*)$$

is convex.

Subgradient

Definition (subgradient)

Given an open set $\Omega \subset \mathbb{R}^d$ and $u : \Omega \to \mathbb{R}$ a convex function, for $x \in \Omega$, the subgradient (subdifferential) of u at x is defined as

$$\partial u(x) := \{p \in \mathbb{R}^n : u(z) \geq u(x) + \langle p, z - x \rangle \ \ \forall z \in \Omega\}.$$

The Brenier potential u is differentiable at x if its subgradient $\partial u(x)$ is a singleton. We classify the points according to the dimensions of their subgradients, and define the sets

$$\Sigma_k(u) := \left\{ x \in \mathbb{R}^d | \ \dim(\partial u(x)) = k \right\}, \quad k = 0, 1, 2 \ldots, d.$$

Regularity of Solution to Monge-Ampere Equation

Theorem (Figalli Regularity)

Let $\Omega, \Lambda \subset \mathbb{R}^d$ be two bounded open sets, let $f, g : \mathbb{R}^d \to \mathbb{R}^+$ be two probability densities, that are zero outside Ω, Λ and are bounded away from zero and infinity on Ω, Λ, respectively. Denote by $T = \nabla u : \Omega \to \Lambda$ the optimal transport map provided by Brenier theorem. Then there exist two relatively closed sets $\Sigma_\Omega \subset \Omega$ and $\Sigma_\Lambda \subset \Lambda$ with $|\Sigma_\Omega| = |\Sigma_\Lambda| = 0$ such that $T : \Omega \setminus \Sigma_\Omega \to \Lambda \setminus \Sigma_\Lambda$ is a homeomorphism of class $C^{0,\alpha}_{loc}$ for some $\alpha > 0$.

Singularity Set of OT Maps

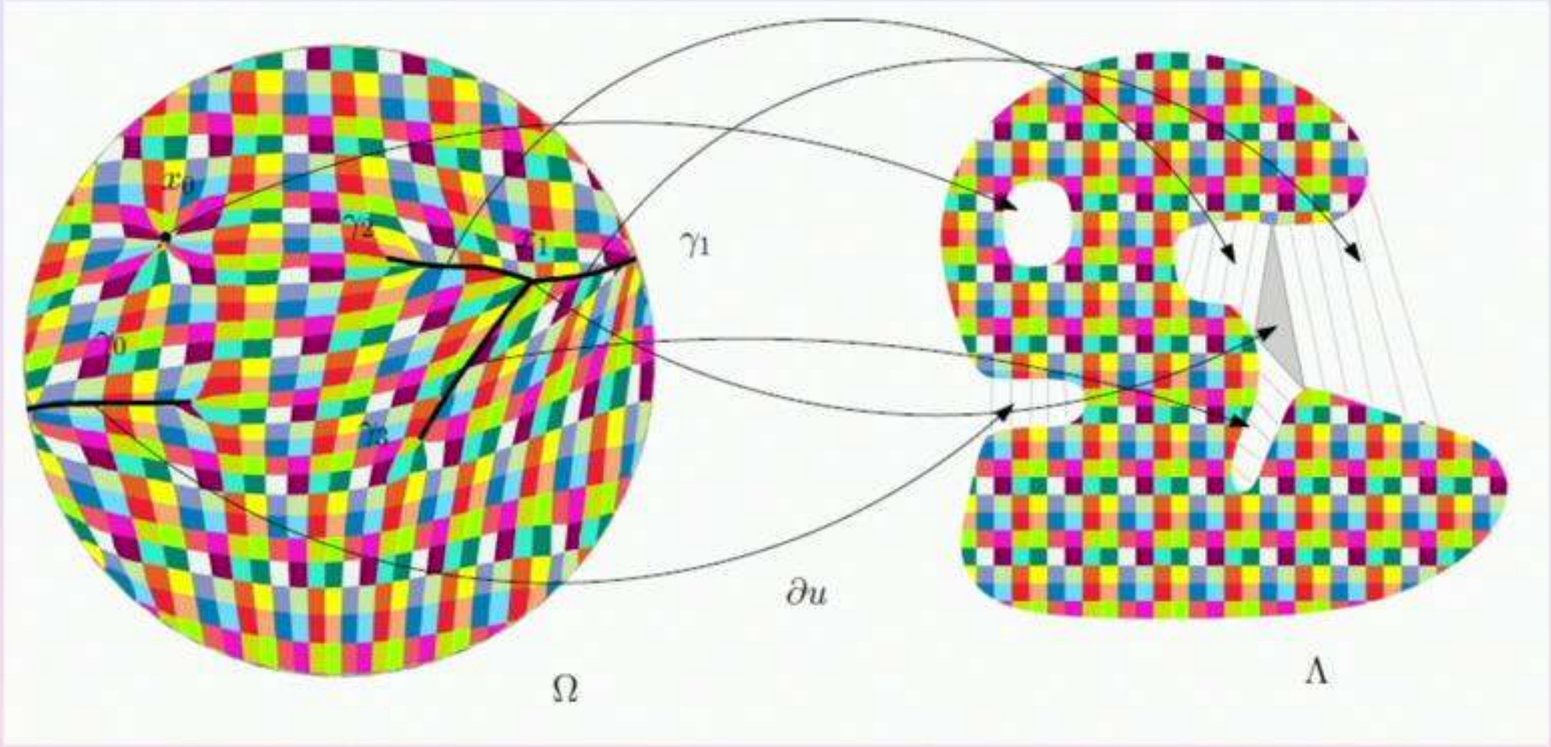

Figure: Singularity structure of an optimal transportation map.

We call Σ_Ω as singular set of the optimal transportation map $\nabla u : \Omega \to \Lambda$.

Discontinuity of Optimal Transportation Map

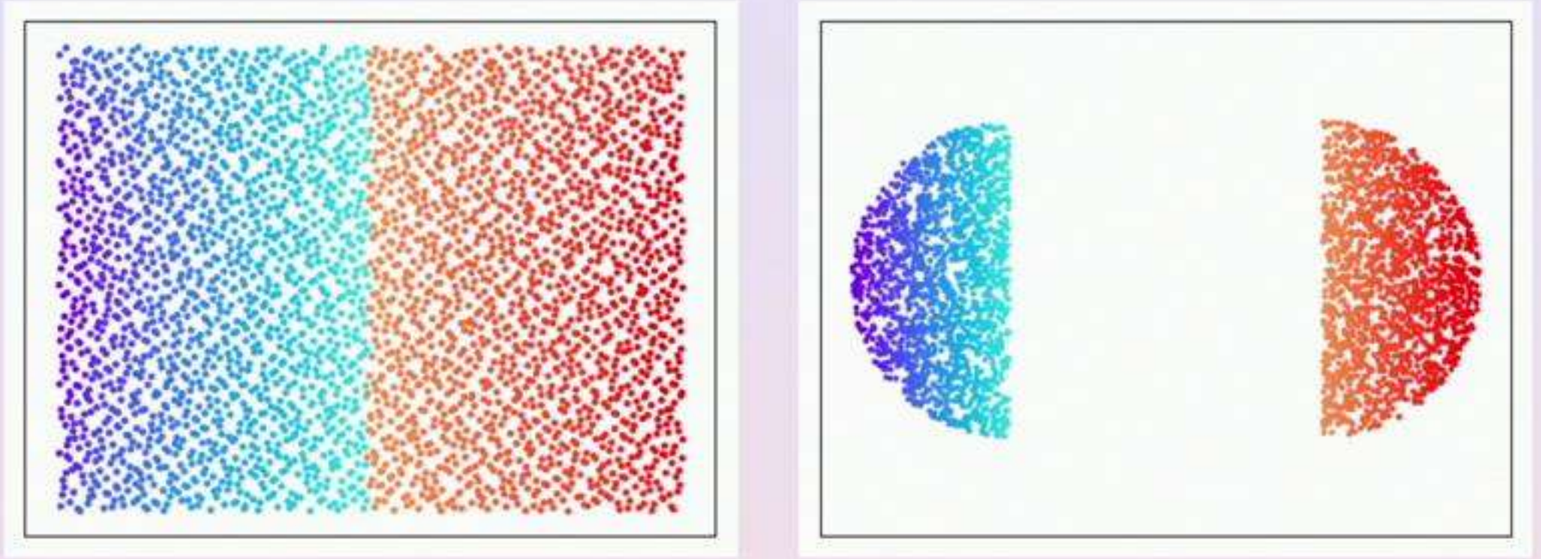

Figure: Discontinuous Optimal transportation map, produced by a GPU implementation of algorithm based on our theorem. The middle line is the singularity set Σ_1.

Discontinuity of Optimal Transportation Map

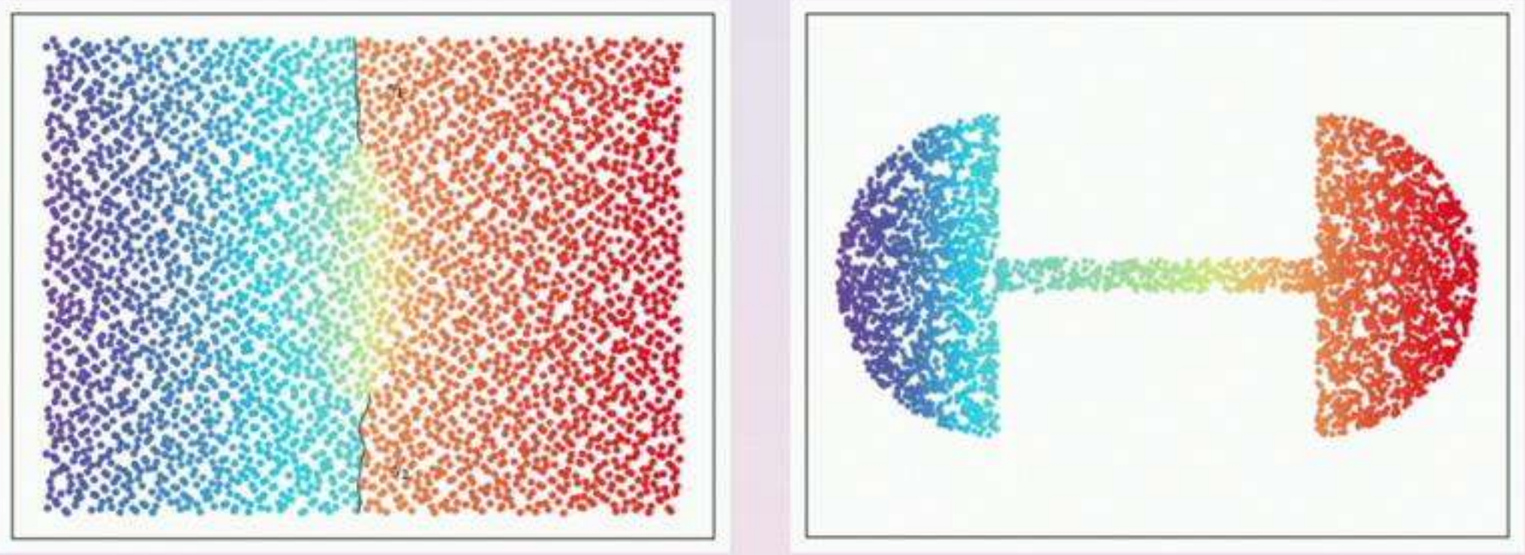

Figure: Discontinuous Optimal transportation map, produced by a GPU implementation of algorithm based on regularity theorem. γ_1 and γ_2 are two singularity sets.

Discontinuity of Optimal Transportation Map

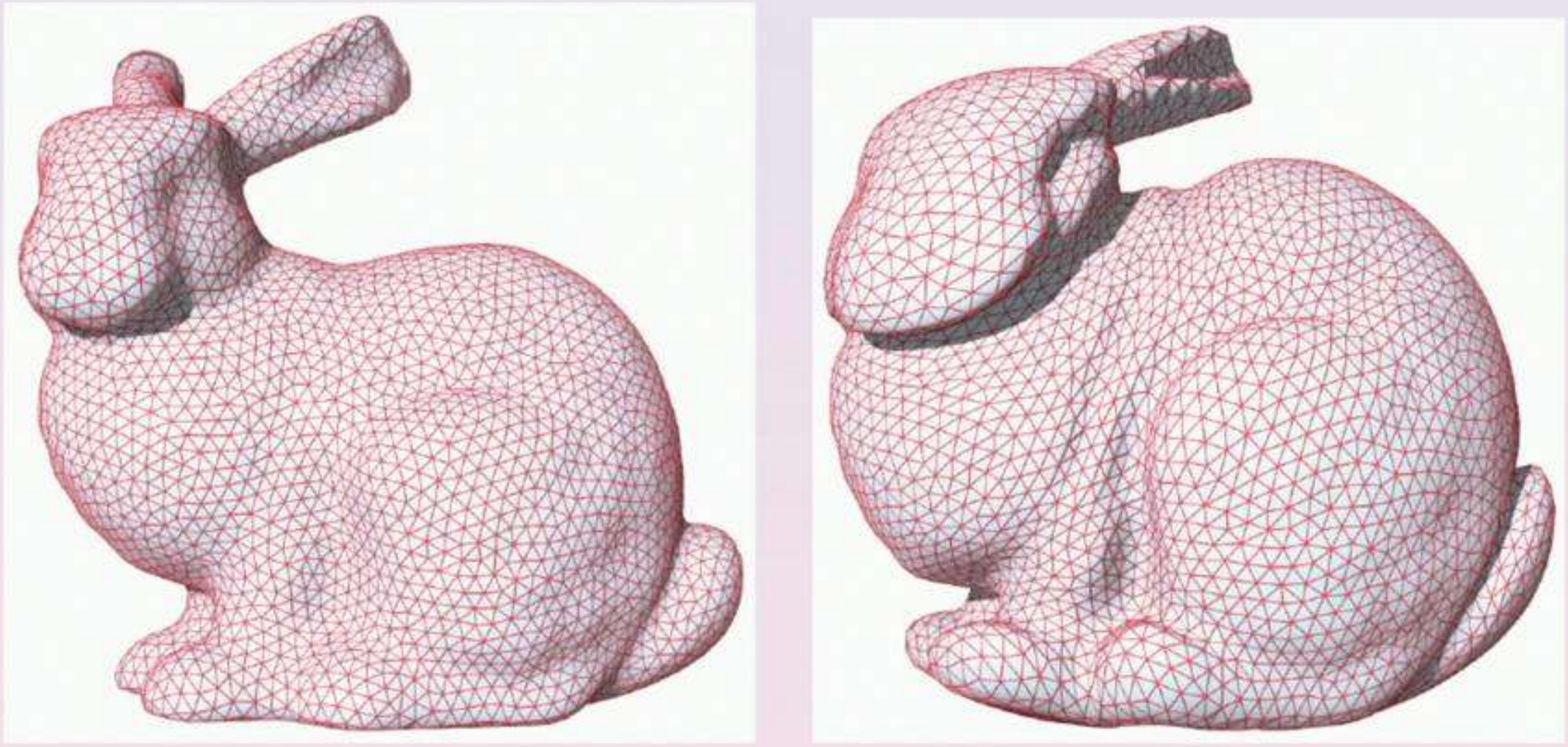

Figure: Optimal transportation between a solid ball to the Stanford bunny. The singular sets are the foldings on the boundary surface.

Discontinuity of Optimal Transportation Map

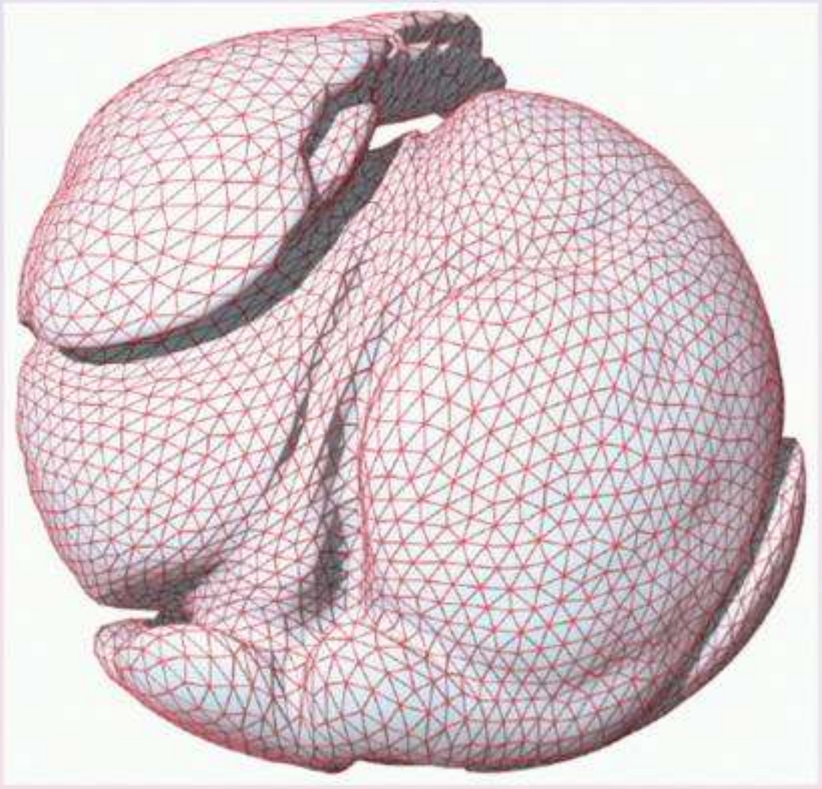

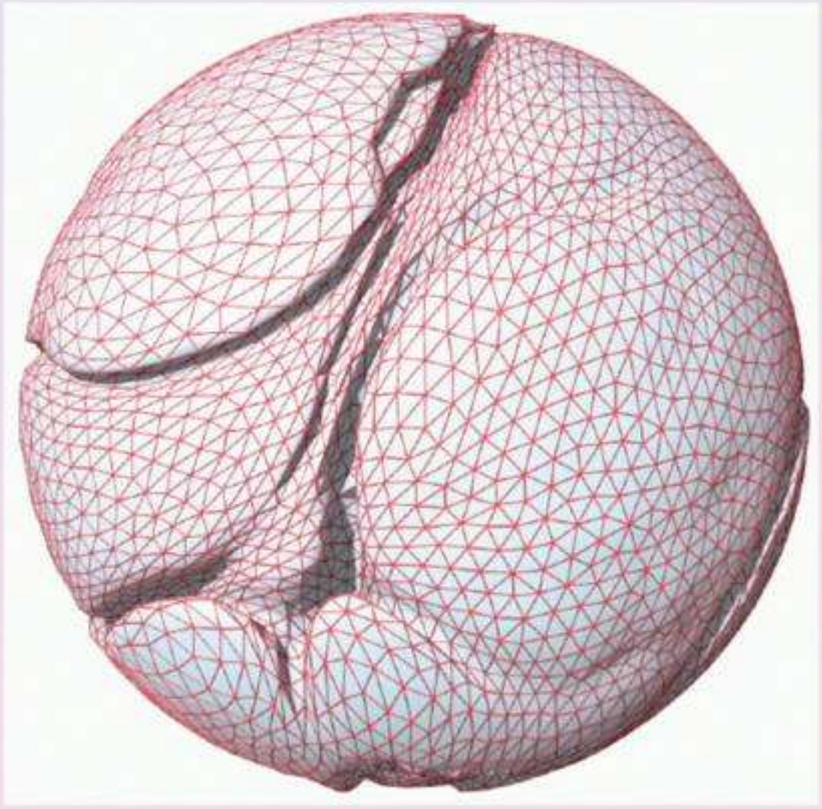

Figure: Optimal transportation between a solid ball to the Stanford bunny. The singular sets are the foldings on the boundary surface.

Discontinuity of Optimal Transportation Map

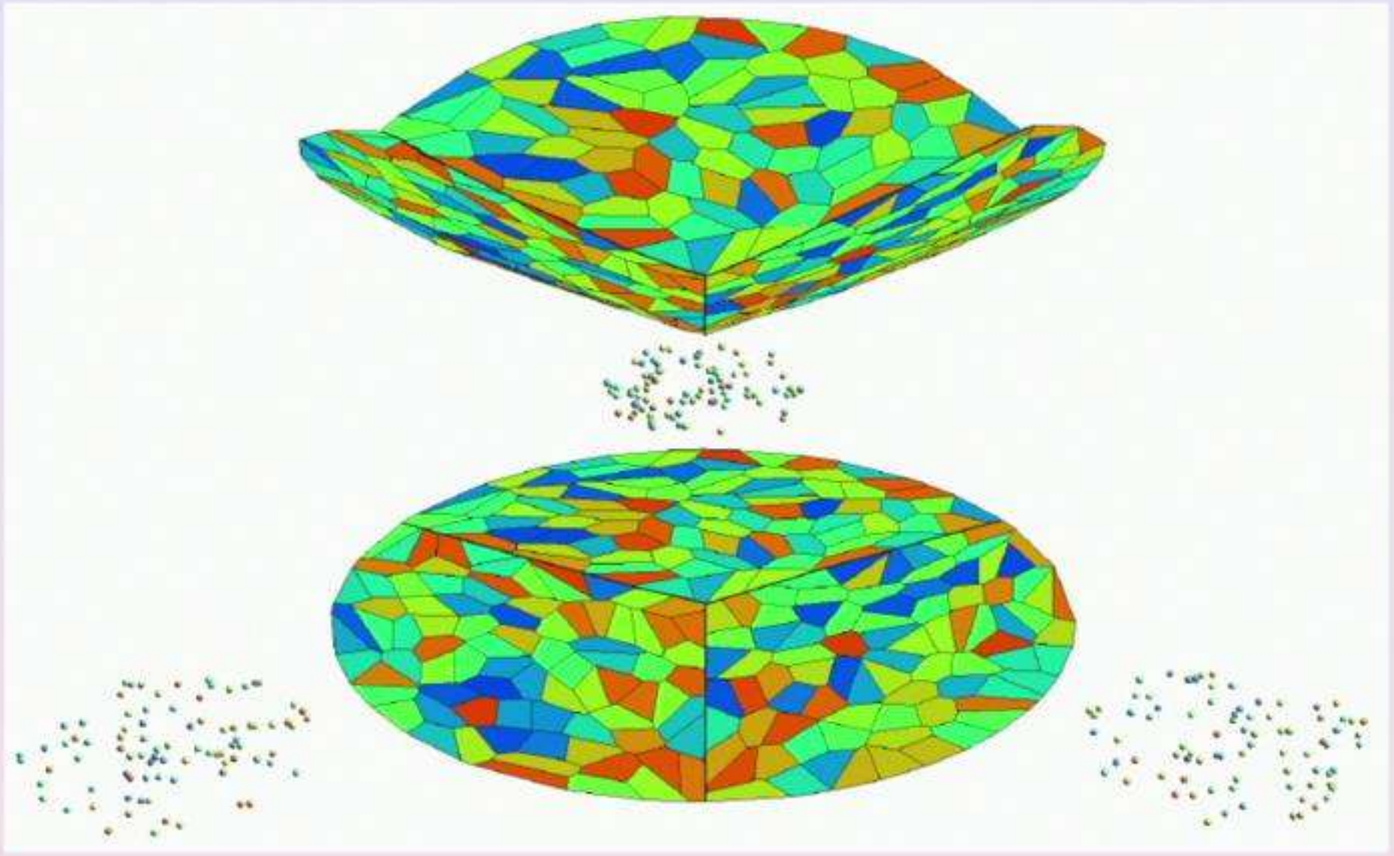

Figure: Optimal transportation map is discontinuous, but the Brenier potential itself is continuous. The projection of ridges are the discontinuity singular sets.

Mode Collapse

Intrinsic Conflict

Deep neural networks can only represent continuous mappings, but the transportation maps are discontinuous on singular sets. Namely, the target mappings are outside the functional space of Dnns. This conflict induces mode collapsing.

Avoid Mode Collapse

The optimal transport map is discontinuous, but Brenier potential itself is continuous. The neural network should represent the Brenier potential, instead of its gradient, namely the transportation map.

Mode Collapse

1. The training process is unstable, and doesn't converge;
2. The searching converges to one of the multiple connected components of Λ, the mapping converges to one continuous branch of the desired transformation mapping. This means we encounter a mode collapse;
3. The training process leads to a transportation map, which covers all the modes successfully, but also cover the regions outside Λ. In practice, this will induce the phenomena of generating unrealistic samples.

Mode Collapse

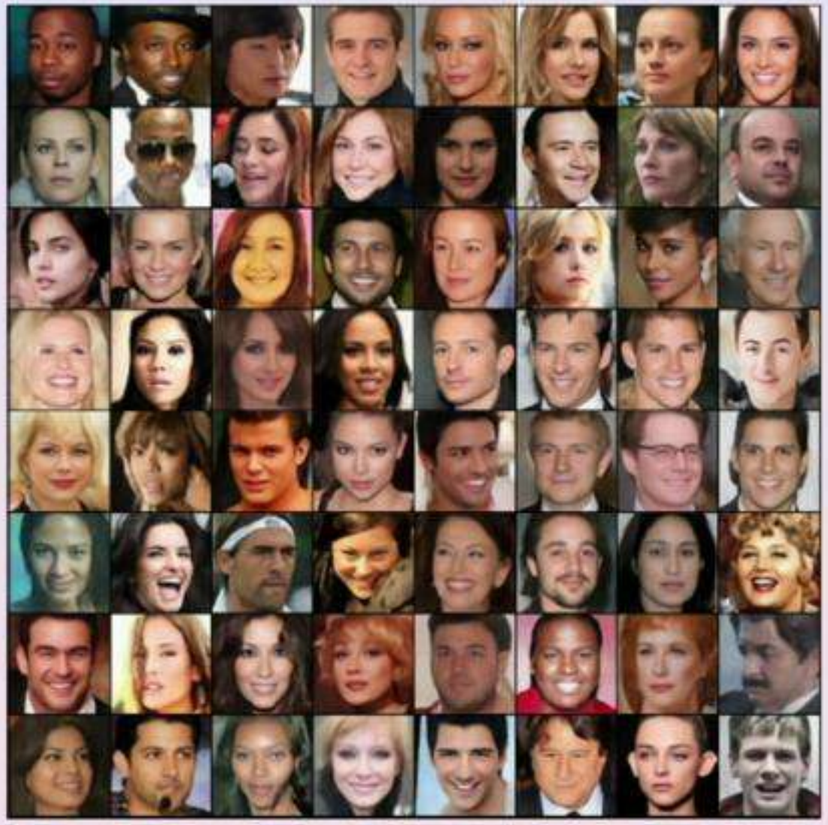

(a) generated facial images

(b) a path through a singularity.

Figure: Facial images generated by an AE-OT model, the image in the center of (b) shows the transportation map is discontinuous.

Autoencoder-Optimal Transportation Framework

Auntoencoder-OMT

Merits

1. Solving Monge-Ampère equation is reduced to a convex optimization, which has unique solution. The optimization won't be trapped in a local optimum;
2. The Hessian matrix of the energy has explicit formulation. The Newton's method can be applied with second order convergence; or the quasi-Newton's method can be used with super-linear convergence. Whereas conventional gradient descend method has linear convergence;
3. The approximation accuracy can be fully controlled by the density of the sampling density by using Monte-Carlo method;
4. The algorithm can be refined to be hierarchical and self-adaptive to further improve the efficiency;
5. The parallel algorithm can be implemented using GPU.

Experiments - mnist

(a) VAE

(b) WGAN

(c) Our model, AE-OT

(d) Our model, AE-OT

Figure: Comparison between conventional models VAE and WGAN with our model AE-OT (AutoEncoder-OptimalTransportation).

Experiments - WGAN-QC CelebA

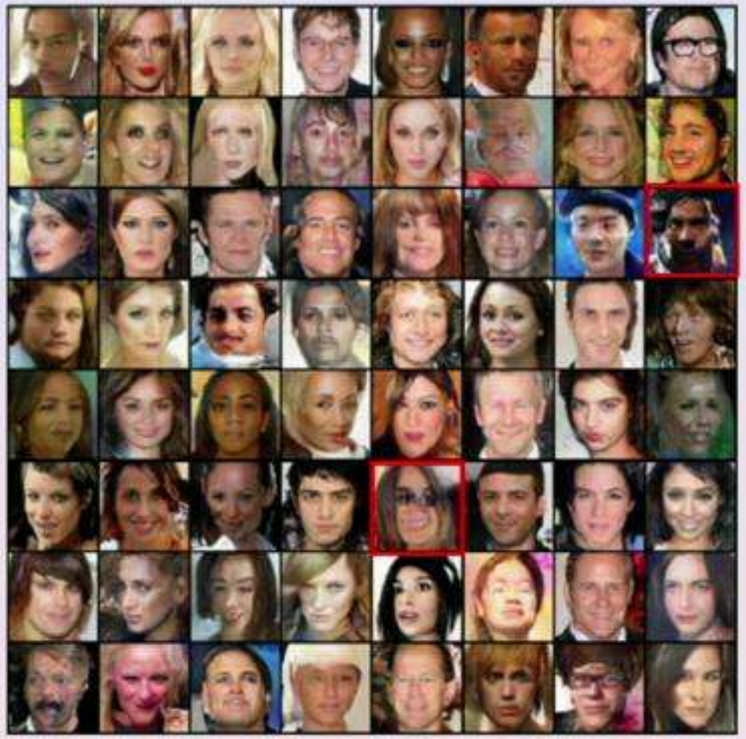

(a) WGAN-GP

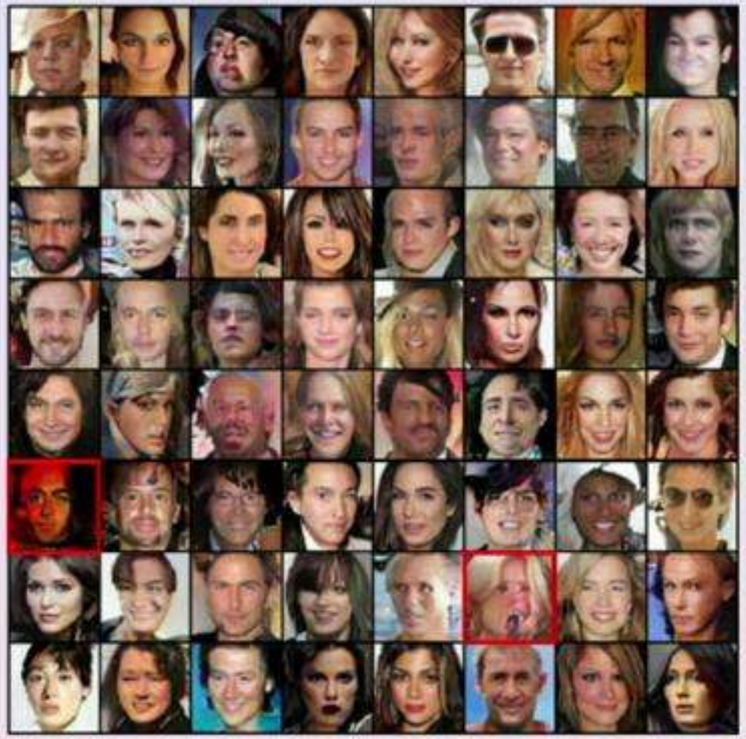

(b) WGAN-div

Figure: Failure cases for WGAN-GP and WGAN-div.

Experiments - WGAN-QC CelebA

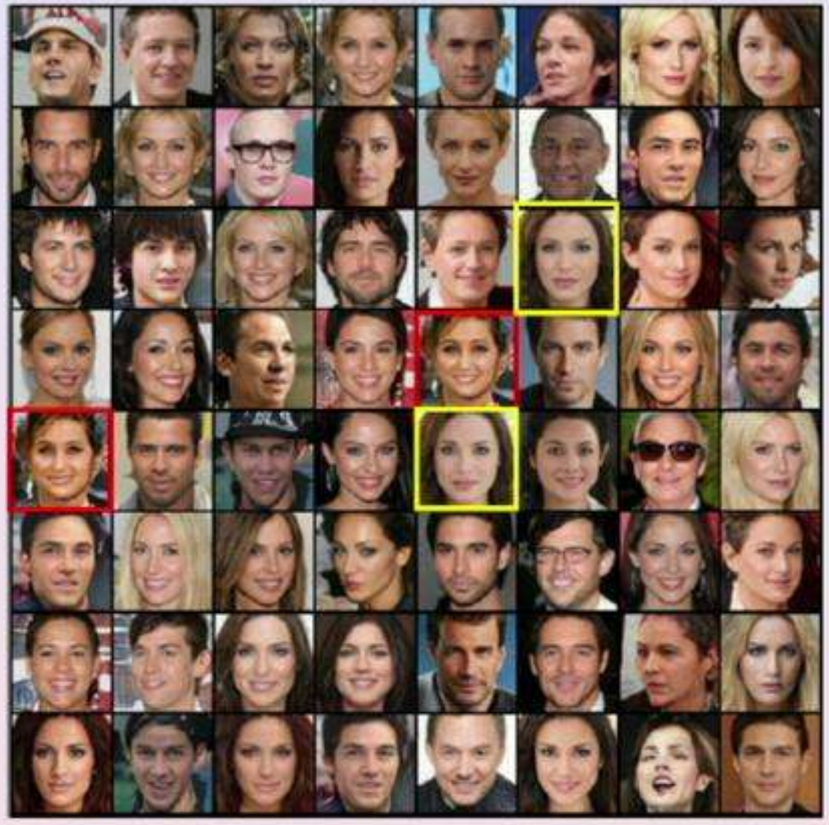

(c) CRGAN - mode collapsing

(d) Our model

Figure: Comparision between CRGAN and our model.

Experiments - AE-OT CelebA

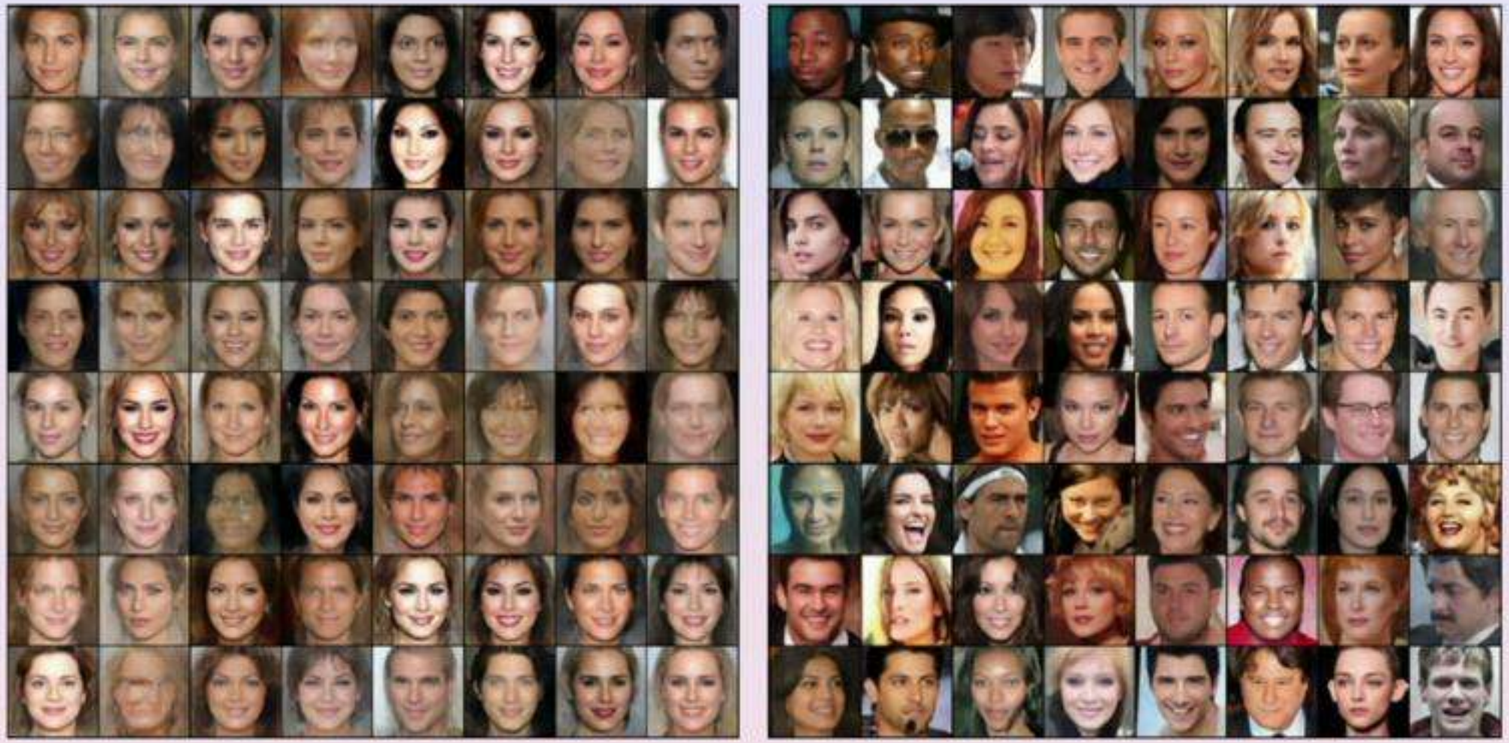

Figure: Human facial images generated by our AE-OT model (AutoEncoder-OptimalTransportation).

Experiments - WGAN-QC CelebAHQ

Figure: Human facial images generated by our model.

Experiments - WGAN-QC CelebAHQ

Figure: Human facial images generated by our model.

Experiments - MNIST Fashion

MM GAN	NSGAN	LSGAN
29.6	26.5	30.7
WGAN	**BEGAN**	**VAE**
21.5	22.9	68.7
GLO	**GLANN**	**AE-OMT**
57.7	13	11.2

Figure: Our method has smallest FID score. (Fréchet Inception Distance)

Conclusion

This work introduces a geometric understanding of deep learning:

- The intrinsic pattern of natural data can be represented by manifold distribution hypothesis.
- The deep learning system has two major tasks: manifold learning and probability distribution transformation.
- Optimal transportation methods can be used to accomplish the second task.
- By Brenier theory, the generator and discriminator should collaborate instead of compete with each other;
- The regularity theory of Monge-Ampere equation explains mode collapse;
- The AE-OT framework can avoid mode collapse, and make half the blackbox transparent.

Thanks

For more information, please email to yau@math.harvard.edu.

Thank you!